

COOLTEMP: A COMPUTER CODE FOR CALCULATING COOLANT TEMPERATURES  
IN EBR-II SUBASSEMBLIES

by

W. R. Wallin, P. E. Blomberg, and J. F. Koenig

EBR-II Project  
Argonne National Laboratory  
Argonne, Illinois - Idaho Falls, Idaho

May 1971

Work performed under the auspices of the U. S. Atomic Energy Commission

This report was prepared as an account of work sponsored by the United States Government. Neither the United States nor the United States Atomic Energy Commission, nor any of their employees, nor any of their contractors, subcontractors, or their employees, makes any warranty, express or implied, or assumes any legal liability or responsibility for the accuracy, completeness or usefulness of any information, apparatus, product or process disclosed, or represents that its use would not infringe privately owned rights.

## **DISCLAIMER**

**This report was prepared as an account of work sponsored by an agency of the United States Government. Neither the United States Government nor any agency Thereof, nor any of their employees, makes any warranty, express or implied, or assumes any legal liability or responsibility for the accuracy, completeness, or usefulness of any information, apparatus, product, or process disclosed, or represents that its use would not infringe privately owned rights. Reference herein to any specific commercial product, process, or service by trade name, trademark, manufacturer, or otherwise does not necessarily constitute or imply its endorsement, recommendation, or favoring by the United States Government or any agency thereof. The views and opinions of authors expressed herein do not necessarily state or reflect those of the United States Government or any agency thereof.**

## **DISCLAIMER**

**Portions of this document may be illegible in electronic image products. Images are produced from the best available original document.**



TABLE OF CONTENTS

	<u>Page</u>
ABSTRACT . . . . .	9
I. INTRODUCTION . . . . .	10
II. CALCULATION PROCEDURE . . . . .	10
A. Subassembly Flow . . . . .	11
B. Subassembly Power . . . . .	12
1. Rows 1-6 . . . . .	13
2. Row 7 . . . . .	15
C. Coolant Temperature at Top of Fuel . . . . .	15
D. Coolant Temperature at Top of Reflector . . . . .	16
E. Temperature of Mixed Coolant . . . . .	16
F. Comparison of Calculated Temperature of Mixed Coolant with Measured Temperature . . . . .	19
G. Average Power and Flow per Element . . . . .	19
III. RESULTS OF USING COOLTEMP . . . . .	23
A. Effect of Flow Correction . . . . .	23
B. Comparison with Results of Power Calculation with Other Codes . . . . .	31
C. Comparison of Calculated Temperatures with Temperatures Measured by Melt Wires . . . . .	31
D. Comparison of Calculated Temperatures with Temperatures Measured by Thermocouples . . . . .	35
IV. CONCLUSIONS . . . . .	57



LIST OF FIGURES

<u>No.</u>	<u>Title</u>	<u>Page</u>
1.	Location of Thermocouples for Measuring Subassembly Outlet Coolant Temperature . . . . .	20
2.	Location of Thermocouples in Relation to Subassembly Positions . . . . .	21
3.	Neutron Radiographs of Melt-wire Temperature Monitor before and after Irradiation; the Four Center Wires Melted during Irradiation . . . . .	34
4.	Comparison of Thermocouple-measured and COOLTEMP-calculated Temperatures for Runs 30A-45B: Grid Position 1A1 . . . . .	37
5.	Comparison of Thermocouple-measured and COOLTEMP-calculated Temperatures for Runs 30A-45B: Grid Position 2A1 . . . . .	38
6.	Comparison of Thermocouple-measured and COOLTEMP-calculated Temperatures for Runs 30A-45B: Grid Position 2B1 . . . . .	39
7.	Comparison of Thermocouple-measured and COOLTEMP-calculated Temperatures for Runs 30A-45B: Grid Position 2C1 . . . . .	40
8.	Comparison of Thermocouple-measured and COOLTEMP-calculated Temperatures for Runs 30A-45B: Grid Position 2D1 . . . . .	41
9.	Comparison of Thermocouple-measured and COOLTEMP-calculated Temperatures for Runs 30A-45B: Grid Position 2E1 . . . . .	42
10.	Comparison of Thermocouple-measured and COOLTEMP-calculated Temperatures for Runs 30A-45B: Grid Position 2F1 . . . . .	43
11.	Comparison of Thermocouple-measured and COOLTEMP-calculated Temperatures for Runs 30A-45B: Grid Position 3B1 . . . . .	44
12.	Comparison of Thermocouple-measured and COOLTEMP-calculated Temperatures for Runs 30A-45B: Grid Position 3C1 . . . . .	45
13.	Comparison of Thermocouple-measured and COOLTEMP-calculated Temperatures for Runs 30A-45B: Grid Position 3E1 . . . . .	46
14.	Comparison of Thermocouple-measured and COOLTEMP-calculated Temperatures for Runs 30A-45B: Grid Position 3F1 . . . . .	47
15.	Comparison of Thermocouple-measured and COOLTEMP-calculated Temperatures for Runs 30A-45B: Grid Position 4B1 . . . . .	48
16.	Comparison of Thermocouple-measured and COOLTEMP-calculated Temperatures for Runs 30A-45B: Grid Position 4C3 . . . . .	49

List of Figures (contd)

<u>No.</u>	<u>Title</u>	<u>Page</u>
17.	Comparison of Thermocouple-measured and COOLTEMP-calculated Temperatures for Runs 30A-45B: Grid Position 4E1 . . . . .	50
18.	Comparison of Thermocouple-measured and COOLTEMP-calculated Temperatures for Runs 30A-45B: Grid Position 4F1 . . . . .	51
19.	Comparison of Thermocouple-measured and COOLTEMP-calculated Temperatures for Runs 30A-45B: Grid Position 4F3 . . . . .	52
20.	Comparison of Thermocouple-measured and COOLTEMP-calculated Temperatures for Runs 30A-45B: Grid Position 5A4 . . . . .	53
21.	Comparison of Thermocouple-measured and COOLTEMP-calculated Temperatures for Runs 30A-45B: Grid Position 5C2 . . . . .	54
22.	Comparison of Thermocouple-measured and COOLTEMP-calculated Temperatures for Runs 30A-45B: Grid Position 6C4 . . . . .	55



LIST OF TABLES

<u>No.</u>	<u>Title</u>	<u>Page</u>
I.	Overall Heat-transfer Coefficients for Radial Heat Transfer in Upper Reflector Section . . . . .	17
II.	Average Powers and Flows per Element Used as AIROS Input for Run 39A . . . . .	22
III.	COOLTEMP Output Data . . . . .	24
IV.	Flow Correction Factor, Measured Instrumented-subassembly Flow, and Pressure Drop: Runs 39A-45B . . . . .	29
V.	Change in Flow Correction Factor, Pressure Drop, and Instru- mented-subassembly Flow . . . . .	30
VI	Power in Subassemblies in Rows 1-6 in EBR-II Run 39A, as Calculated by Three Codes . . . . .	32
VII.	Comparison of Calculated Top-of-reflector Temperatures with Temperatures Measured by Melt Wires . . . . .	36



COOLTEMP: A COMPUTER CODE FOR CALCULATING COOLANT TEMPERATURES  
IN EBR-II SUBASSEMBLIES

by

W. R. Wallin, P. E. Blomberg, and J. F. Koenig

ABSTRACT

COOLTEMP is a FORTRAN IV computer code that has been developed for use on the IBM 360/75 computer to calculate flow rate, power, and coolant temperature of each subassembly in rows 1-7 of EBR-II. The temperatures calculated are average values at three points above the core. The code is used to predict temperatures for 19 subassembly locations where outlet temperatures are measured by thermocouples. Signals from these thermocouples are used to initiate alarm and, in a few cases, shutdown circuits. Changes in reactor loading resulting from installation of experiments in the reactor cause considerable variation in the temperatures measured.

Power in each subassembly, as calculated by COOLTEMP, agrees within a few percent of the power calculated by other codes, except for a few cases where the difference is a maximum of 10%. Flow is believed to be calculated to an accuracy of better than 10%, although comparison with flow measurements in an instrumented subassembly indicated a 12% difference. Subassembly outlet temperature, as measured by the thermocouple, is predicted within about 13°F for the central core position (i.e., a maximum error of about 10% in the 135°F temperature rise in the subassembly). Although power and flow in experimental-irradiation subassemblies may be as much as 90% less than in a normal driver subassembly, the effects of loading changes are represented fairly well. Work is continuing to improve the accuracy of the results.

## I. INTRODUCTION

EBR-II was designed as a power demonstration reactor. To monitor the performance of the fuel subassemblies in the reactor, 19 thermocouples were placed just above a representative group of core positions. Early in the power operation, it became apparent that the coolant temperatures measured for positions in rows 5 and 6 were not the expected values. As the function of the reactor was changed to testing of fuels and materials, experimental-irradiation subassemblies replaced subassemblies containing reference-design fuel elements, and the discrepancy between expected and measured temperatures increased.

COOLTEMP was developed to predict measured reactor coolant temperatures more closely. It is a FORTRAN IV computer code used on the IBM 360/75 computer to calculate flow rate and power, and from these, the coolant temperature, in each subassembly in rows 1-7 of EBR-II. The temperatures calculated are average values at three points above the core. Since experiments that have widely differing performance characteristics may be placed in almost any grid position, power and flow rate for each grid position has to be determined. Radial heat transfer between adjacent subassemblies also has to be determined.

Setpoints for shutdown trips and alarms must be established for each reactor run. The goal of the program is to establish these values more precisely before initial startup for the run. COOLTEMP calculations have been helpful in establishing the setpoints, but the accuracy is not good enough yet to rely on the calculated values alone. Estimates based on previous similar loading conditions are now used.

## II. CALCULATION PROCEDURE

COOLTEMP calculations are divided into three major parts. The flow rate in each subassembly is determined first. Then, the power in each subassembly is calculated based on specific power for gamma absorption and fission. Finally, the coolant temperature for each subassembly is calculated in three steps. Coolant temperature at the top of the fuel first is calculated from subassembly flow rate and power. Next, the coolant

temperature at the top of the subassembly upper reflector region is calculated by adding the effect of radial heat transfer to the calculated coolant temperature at the top of the fuel. Then, the "mixed-coolant" temperature is calculated by adding to the top-of-reflector temperature a correction factor for the effect of mixing the coolant with coolant from adjacent subassemblies.

COOLTEMP also calculates the difference between the calculated mixed-coolant temperature and the thermocouple-measured temperature.

A. Subassembly Flow

In the initial design of EBR-II fuel, all driver subassemblies were to have the same amount of fissionable material, and blanket subassemblies in rows 6 and 7 contained depleted uranium. To limit the differences between coolant temperatures throughout the reactor, which could be caused by power production being lower at the edge of the core than at the center, an orificing system was provided to ensure higher coolant flow rates toward the core center. Although subassemblies in rows 1-7 all take their flow from a common plenum and discharge their flow to a common plenum, the effective pressure drop is different for each row. Subassembly pressure drop was measured in a 0.6-scale model of the reactor and was found to vary with row. With the reference-design core (no experiments), the pressure drops (in psi) were:

Row-1 and -2 subassemblies	37.9
Row-3 subassemblies	38.8
Safety-rod subassemblies	39.0
Row-4 subassemblies	34.6
Row-5 subassemblies	34.2
Control-rod subassemblies	38.8
Row-6 and -7 subassemblies	40.8

These values are based on a flow of 7620 gpm for rows 1-7 and a differential pressure of 46.2 psi between the pump discharge and the upper (discharge) plenum of the reactor.

The flow rate for any subassembly is governed by the size of the holes (orifices) in the lower adapter of the subassembly and by the row in

which the subassembly is installed. The grid plate supporting the subassemblies is stepped so that the holes are exposed to varying degrees depending on the row in which the subassembly is installed.\*

The relationship of flow rate to pressure drop for each experimental-irradiation subassembly and for typical driver and blanket subassemblies is determined in a water test loop. The values obtained are converted to sodium conditions at 800°F. The relationship determined from the flow test is used to determine the flow rate for the pressure drop at the core position where the subassembly will be installed. This flow rate is called the "calibrated flow."

The calibrated flow for the subassemblies is summed for the first seven rows. The flow for each subassembly is then corrected by a flow correction factor, which is the ratio of the measured core flow (rows 1-7) to the sum of the calibrated flows. Measured core flow is kept at the same value for each run; the reactor operators control the total outlet flow to maintain a constant 9000 gpm.

When the effective pressure drops for each row were originally determined, they were based on the conditions at the time, i.e., equal flow for each subassembly of a given type in a given row. No experimental-irradiation subassemblies were anticipated. However, some experimental-irradiation subassemblies now in the reactor are designed for flows approaching 1% of the flow in surrounding subassemblies, and therefore provide more resistance to flow. Flow division between parallel channels connecting two plenums is not theoretically well understood, especially when the parallel channels have differing flow resistances. To arrive at the flow for each position as it changes from run to run, the pressure drop would have to be known for each core position. Since this information is not available, the flow correction factor described above is applied to each core position.

#### B. Subassembly Power

Powers in the subassemblies in rows 1-6 are calculated separately from

---

\* L. J. Koch, W. B. Loewenstein, and H. O. Monson, Addendum to Hazard Summary Report, Experimental Breeder Reactor-II (EBR-II), ANL-5719 (Addendum), Figs. 11-15 (June 1962).

those in row 7. Different constants for the specific powers due to  $^{238}\text{U}$  fission and to gamma absorption must be used.

The equations that follow are based on 50 MWt, the operating reactor power level when COOLTEMP was first put into use. To calculate the power in each subassembly at other reactor power levels, the constants for specific power must be changed. However, after the power in a subassembly has been calculated at one reactor power level, it can easily be determined for other power levels, because subassembly power varies linearly with reactor power.

# 1. Rows 1-6

The power in each subassembly for a reactor power of 50 MWt is calculated by COOLTEMP, in terms of specific powers due to fissions and gamma absorption, by the equation

$$P^{(xyz)} = \phi^{(xyz)} [K_f M_f^{(xyz)} + K_1 M_u^{(xyz)} + K_3 (M_u^{(xyz)} - M_f^{(xyz)}) + K_2 M_c^{(xyz)}], \quad (1)$$

- where  $P^{(xyz)}$  = Power in subassembly (W);  
 $\phi^{(xyz)}$  = Relative radial flux in subassembly;  
 $K_f$  = Specific power due to fissions in fissionable material (W/g);  
 $M_f^{(xyz)}$  = Total mass of fissionable material ( $^{235}\text{U} + ^{239}\text{Pu} \times 1.2$ ) in subassembly (g);  
 $K_1$  = Specific power due to gamma absorption in fissile and fertile material at core center (8.9 W/g\*);  
 $M_u^{(xyz)}$  = Total mass of fissile and fertile materials (uranium and plutonium) in subassembly (g);  
 $K_3$  = Specific power due to fissions in  $^{238}\text{U}$  at core center (16.9 W/g\*);  
 $K_2$  = Specific power due to gamma absorption in structural materials and coolant at core center (3.6 W/g\*); and  
 $M_c^{(xyz)}$  = Total mass of structural materials and coolant (stainless steel and sodium) in subassembly (g).

---

\*From Guide for Irradiation Experiments in EBR-II, Rev. 3 (July 1969).

Total reactor power ( $P_t$ ), in kW, is determined from measured values according to the equation

$$P_t = F \cdot \Delta T \cdot K_5, \quad (2)$$

where  $F$  = Sum of readings of four inlet flowmeters minus 105, the leakage to the primary tank between flowmeters and subassembly inlets (gpm),

$\Delta T$  = Reactor outlet temperature minus bulk sodium temperature measured at the inlet to the primary pumps ( $^{\circ}\text{F}$ ), and

$K_5$  = Conversion constant (0.039).

To evaluate  $K_f$ , the total reactor power ( $P_t$ ) is multiplied by the fraction of  $P_t$  generated in rows 1-6 (as determined by the BURNUP code\*), and the product is set equal to the sum of individual powers for subassemblies in rows 1-6 in terms of  $K_f$ :

$$(P_t)_{FP}^{(xyz)} = \sum_{1-6} P^{(xyz)}, \quad (3)$$

where  $P^{(xyz)}$  = Power in a subassembly in terms of  $K_f$ , and

$FP^{(xyz)}$  = Fraction of total power ( $P_t$ ) in all subassemblies considered (rows 1-6).

After the value of  $K_f$  has been determined, the actual power in each subassembly is calculated using Eq. 1.

Relative radial flux,  $\phi^{(xyz)}$ , is obtained from the BURNUP code, which calculates the relative  $^{235}\text{U}$  fission rate in each subassembly position; the fluxes corresponding to those rates are used for  $\phi^{(xyz)}$ . The fission-rate distribution is described by a fourth-order polynomial equation. The five coefficients for this equation are established from experimentally determined flux distributions, using a curve-fitting routine. The asymmetry caused by replacing standard fuel elements with experiments is then considered by calculating the shift of flux center, as determined from measured worths of control rods. Gamma-heating rates and  $^{238}\text{U}$ -fission-heating rates are assumed to have the same distribution.

Fraction of total reactor power,  $FP^{(xyz)}$ , also obtained from the BURNUP code, is based on heat production in fissionable and fertile material. All heat produced (200 MeV per fission) is considered to be due to fission,

---

\* S. M. Masters, I. A. Engen, and F. S. Kirn, BURNUP--A Code to Calculate Burnup of EBR-II Fuel, ANL/EBR-009 (February 1970).



neutron capture, and beta and gamma reactions. Heating produced in structural materials and the coolant is assumed to be small enough to be insignificant in the BURNUP code.

COOLTEMP, however, takes into account gamma heating in structural materials and the coolant, because some experimental-irradiation sub-assemblies contain only structural materials. The amount of this heating in structural-materials experiments must be calculated in order to calculate the coolant temperatures.

## 2. Row 7

Actual power in each row-7 subassembly is calculated by the equation

$$P^{(xyz)} = \frac{\phi^{(xyz)} [K_f M_f^{(xyz)} + K_x K_f M_u^{(xyz)} + K_6 (M_u^{(xyz)} - M_f^{(xyz)}) + K_7 M_c^{(xyz)}]}{(P_t)_{FP}^{(xyz)}}, \quad (4)$$

where  $K_x$  = Specific power due to fissions in  $^{238}\text{U}$  in row 7 (W/g). There are six subassembly positions in each sector, and  $K_x$  has the following values for those positions: 7N1, 0.0118; 7N2, 0.0275; 7N3, 0.0352; 7N4, 0.0369; 7N5, 0.0352; 7N6, 0.0275.

$K_6$  = Specific power due to gamma absorption in fissile and fertile material in row 7 (3.05 W/g<sup>\*</sup>).

$K_7$  = Specific power due to gamma absorption in structural materials and coolant in row 7 (0.613 W/g<sup>\*</sup>).

## C. Coolant Temperature at Top of Fuel

With the power and flow rate for a given subassembly known, the average temperature,  $T^{(xyz)}$ , of the sodium at the top of the fuel in the sub-assembly is calculated by the equation

$$T^{(xyz)} = T_B + P^{(xyz)} / F^{(xyz)} K_5, \quad (5)$$

---

\*From Guide for Irradiation Experiments in EBR-II, Rev. 3 (July 1969).

where  $T_B$  = Temperature of coolant at inlet of subassembly, the bulk sodium temperature ( $^{\circ}\text{F}$ ),  
 $F^{(\text{xyz})}$  = Corrected flow in each subassembly (gpm), and  
 $K_5$  = Conversion constant (0.039).

D. Coolant Temperature at Top of Reflector

The coolant temperature at the top of the reflector is determined by considering the amount of radial heat transfer in the upper reflector section. All coolant at the top of the fuel in the subassembly is assumed to be at the same temperature. From the calculated temperatures at the top of the core and the overall heat-transfer coefficients from Table I, the temperatures at the top of the reflector are obtained by iterative calculation. In general, the radial heat transfer becomes important only for low-flow experiments. For driver subassemblies, the overall heat-transfer coefficients include the effect of the nonsymmetrical resistance of the stainless trifiute reflector. The assumption of uniform coolant temperature is valid for the driver subassemblies, in which the coolant mixes in a plenum a short distance above the core region. In the experimental subassemblies, the fuel elements extend to the top of the subassembly, and the coolant in each channel remains essentially at its top-of-fuel temperature. As the outside channels are cooler than the inner channels, because of the higher ratio of flow area to heat-transfer area, the coolant temperature adjacent to the wall will be less than the average coolant temperature in the subassembly. Since the amount of radial heat transfer will be determined by the coolant temperature adjacent to the outside wall, it will be underestimated for experiments whose mixed-coolant temperature is lower than that of the surrounding subassemblies. Similarly, the amount of radial heat transfer from an experiment whose mixed-coolant temperature is higher than that of the surrounding subassemblies will be overestimated; the radial heat transfer may actually add heat to the experiment rather than remove it.

E. Temperature of Mixed Coolant

Comparison of measured temperatures and calculated top-of-reflector temperatures indicated that temperatures in adjacent subassemblies affect the

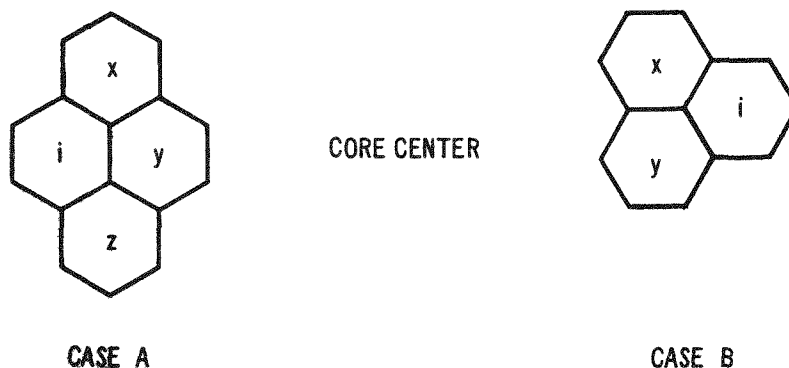
TABLE I. Overall Heat-transfer Coefficients for Radial Heat  
Transfer in Upper Reflector Section

<u>Type of Subassemblies Involved</u>	<u>Coefficient, Btu/hr-°F</u>
Mark-IA Driver to Mark-IA Driver	209
Mark-IA Driver to Control Rod	161
Mark-IA Driver to Mark-A <sup>a</sup> Experiment	163
Mark-IA Driver to Mark-B Experiment	209
Control Rod to Mark-A Experiment	180
Control Rod to Mark-B Experiment	205
Mark-A Experiment to Mark-A Experiment	229
Mark-B Experiment to Mark-B Experiment	409
Mark-A Experiment to Mark-B Experiment	254

---

<sup>a</sup>In a Mark-A experiment, each element is surrounded by a shroud tube. A Mark-B experiment has some unshrouded elements.

thermocouple output. An enthalpy-mixing model has been developed as part of COOLTEMP to describe mixing by radial flow of coolant. It is based on the assumptions of (a) uniform radial flow and (b) mixing of enthalpy from subassemblies located adjacent to the subassembly and toward the center of the core. Coolant from the adjacent interior subassemblies mixes with the coolant from the subassembly in determining a mixed-coolant outlet temperature. Two geometry cases are used in the following to explain the procedure for calculating this temperature:



The enthalpy balance for each case, with 0°F as a basis, is

$$T_{im} CA \left[ F_i + \frac{F_x}{f_x} + \frac{F_y}{f_y} + \frac{F_z}{f_z} \right] = T_i CAF_1 + T_{xm} CA + \frac{F_x}{f_x} + T_{ym} CA \frac{F_y}{f_y} + T_{zm} CA \frac{F_z}{f_z}, \quad (6)$$

where  $T$  = Temperature (°F),

$C$  = Specific heat (Btu/lb-°F),

$A$  = Conversion factor for converting gpm to lb/hr,

$F$  = Subassembly flow (gpm),

$f$  = Fraction of flow to adjacent subassembly;

and the subscripts refer to:

$m$  = Mixed coolant,

$i, x, y, z$  = Subassembly designation.

Solving Eq. 6 for the mixed-outlet coolant temperature,  $T_{im}$ , we have

$$T_{im} = \frac{T_i F_i + T_{xm} \frac{F_x}{f_y} + T_{ym} \frac{F_y}{f_y} + T_{zm} \frac{F_z}{f_z}}{F_1 + \frac{F_x}{f_x} + \frac{F_y}{f_y} + \frac{F_z}{f_z}}.$$

The mixed-coolant outlet temperature is considered to be a function of the flow and the outlet coolant temperature of subassembly i as well as flow and outlet temperature of the adjacent interior subassemblies. For Case A, the values currently used for factor f are 4 for x and z and 2 for y. For Case B, 2 is used for both x and y.

The calculated mixed-coolant temperatures and measured temperatures are in good agreement for some subassemblies. The model, however, does not predict the measured outlet coolant temperature for all positions or for all loading changes. Work is continuing on evaluating different concepts.

One factor considered in this mixing effect was the position of the thermocouple. Figure 1 shows typical placement of a thermocouple. In order to place the thermocouple as close as possible to the subassembly outlet (about 1/4 in. from it), the thermocouple is not centered on a subassembly, but is near one side. The side is not always the same with respect to core center. Figure 2 shows a plan view of the subassembly positions and the thermocouple positions.

The thermocouple position would seem to be especially important when the thermocouple is next to an adjacent subassembly in which the flow rate is greatly different. Attempts to analyze relationships between flow, thermocouple position, and measured temperatures have not produced any consistent correlation.

F. Comparison of Calculated Temperature of Mixed Coolant with Measured Temperature

The final step in the COOLTEMP code is to take the difference between the calculated mixed-coolant temperature and the measured (by thermocouple) temperature.

G. Average Power and Flow per Element

An auxiliary subroutine calculates the average power and the average flow per element. The calculation considers one row at a time and separates the experiments and the driver subassemblies. Table II shows a typical output.

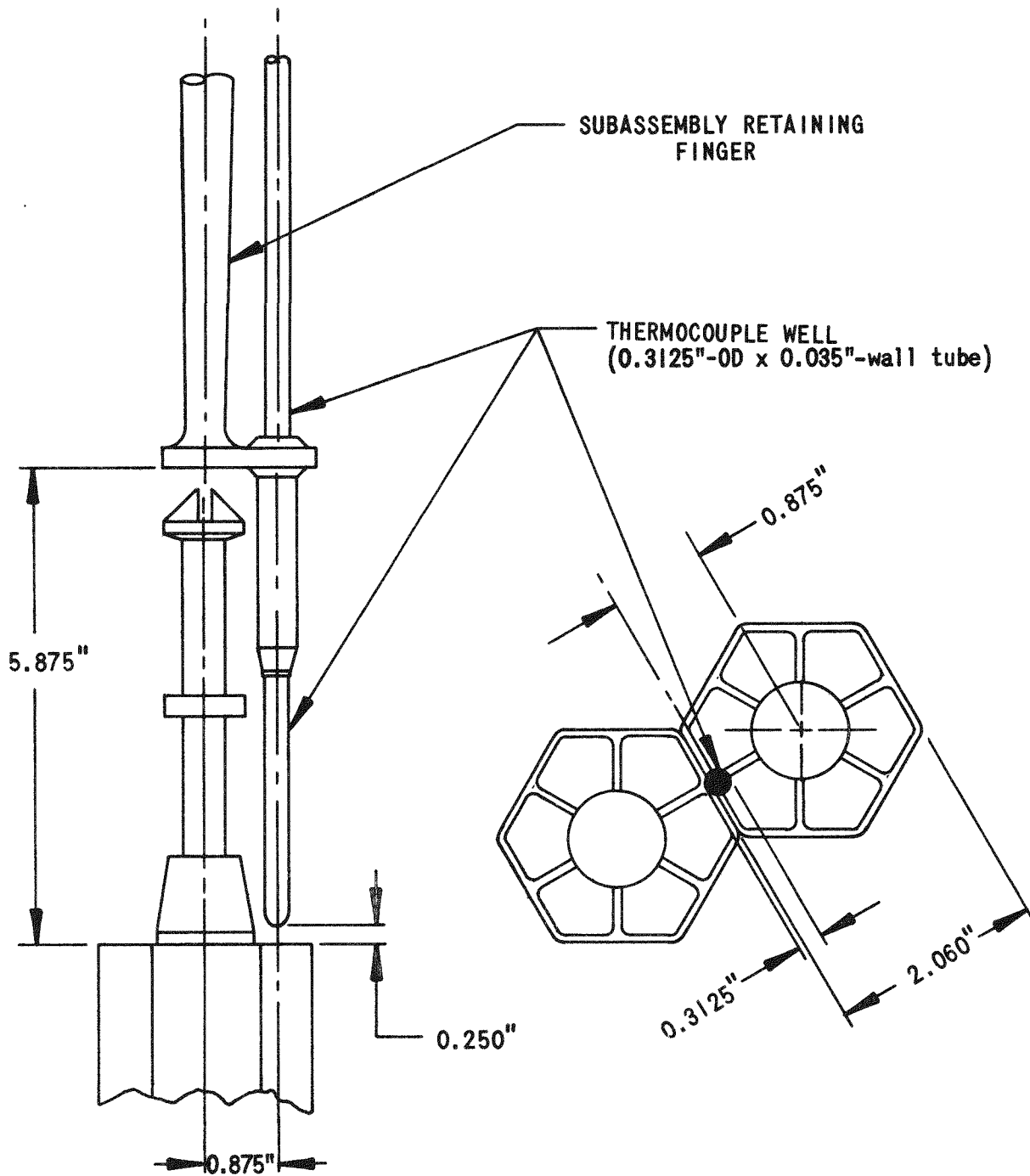


Fig. 1. Location of Thermocouples for Measuring Subassembly Outlet Coolant Temperature

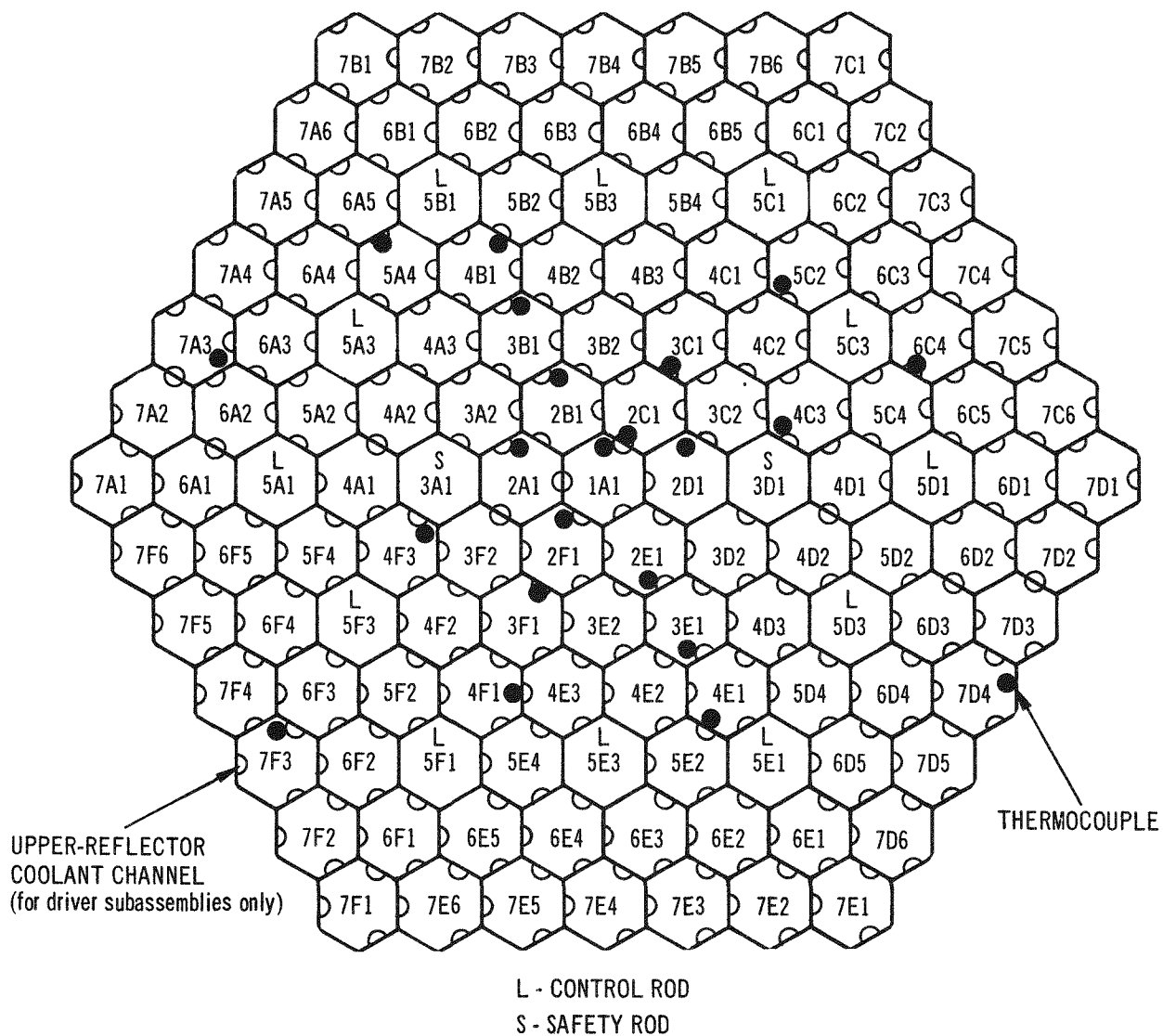


Fig. 2. Location of Thermocouples in Relation to Subassembly Positions

TABLE II. Average Powers and Flows per Element Used as  
AIROS Input for Run 39A

Row No.	Type of Subassembly	Number of Subassemblies	Number of Elements	Average Power per Element, kW	Total Flow, gpm	Average Flow per Element, gpm
1	Driver	1	91	8.56	157.7	1.7
	Experiment	0	--	--	--	--
2	Driver	3	273	8.37	253.9	0.9
	Experiment	3	21	3.33	39.8	1.9
3	Driver	9	819	7.69	958.7	1.2
	Experiment	3	159	7.52	256.7	1.6
4	Driver	9	819	7.48	916.2	1.1
	Experiment	9	231	12.07	526.9	2.3
5	Driver	10	910	6.69	861.4	0.9
	Experiment	14	704	7.34	866.1	1.2
6	Driver	24	2184	5.35	1785.4	0.8
	Experiment	6	168	10.80	276.1	1.6
7	Driver	0	--	--	--	--
	Experiment <sup>a</sup>	36	572	4.04	730.0	1.3

---

<sup>a</sup>Includes blanket subassemblies.



The data obtained are used as input for the AIROS code, a code that simulates reactor dynamics to obtain temperatures, reactivity effects, etc. during transient conditions.

### III. RESULTS OF USING COOLTEMP

The code has been used regularly to predict subassembly outlet temperatures before operating with any given core loading. After measured temperatures at full power are available, the problem has been resubmitted to provide data for analysis of the code's effectiveness and for a long-term historical record of performance. COOLTEMP has been used to solve problems for all reactor runs from run 26 to the present. In addition, it has been used to solve problems for runs 15, 17, 20, and 24. The data presented here are for the period of operation from run 30 through run 45, a period when full power was nominally 50 MWt. Table III is a typical COOLTEMP output.

The results of COOLTEMP are compared with other codes and measured data from instrumented subassemblies, melt-wire capsules, etc. in this section of the report.

#### A. Effect of Flow Correction

For all runs, the sum of calibrated flows was less than the reference-design sum of calibrated flows. The flow correction for run 38A, the run closest to reference-design flow conditions, was only 1%. The highest flow correction was 15%.

Two measured flows can be compared with the flows calculated by COOLTEMP. Instrumented subassemblies with flowmeters were operating in the reactor during runs 39A-45B. Measured changes in flow in these subassemblies should correspond to changes in flow calculated with COOLTEMP. Pressure drop is measured between the discharge of the primary pumps and the upper plenum of the reactor. Although the pressure drop across each subassembly position is not the same, changes in the measured pressure drop from pump discharge to upper plenum should correspond to subassembly flow changes calculated with the code.

TABLE III. COOLTEMP Output Data

CASE 1 RUN: 39A DATE: 3/23/71 TIME: 1741. HOURS TOTAL MEASURED POWER: 49756.3 KW  
 TOTAL COMPUTED POWER: 46596.0 KW COMPUTED POWER, ROWS 1-6: 44283.4 KW COMPUTED POWER, ROW 7: 2312.6 KW  
 TOTAL CALIBRATED FLOW: 6870.4 GPM CORE DIFFERENTIAL PRESSURE: 42.0

POSITION	EXPERIMENT	CALCULATED FLOW (GPM)	REACTOR POWER (IN KW)	COOLANT TEMPERATURE (TOP OF FUEL)	COOLANT TEMPERATURE (TOP OF BLANKET)	CALCULATED MIXED COOLANT TEMPERATURE	MEASURED COOLANT TEMPERATURE	DIFFERENCE BETWEEN MEASURED AND CALCULATED MIXED COOLANT TEMPERATURES
1A1	D	157.7	786.6	831.6	833.3	833.3	822.0	11.32
2A1	D-CF	85.0	773.7	940.1	928.5	906.0	896.0	10.05
2B1	X057	13.0	20.7	742.0	816.5	827.8	814.0	13.78
2C1	D-CF	83.9	766.8	941.1	931.3	907.9	914.0	-6.10
2D1	X021	13.4	24.5	748.1	819.4	828.6	864.0	-35.39
2F1	D-CF	85.0	768.7	938.6	926.5	904.5	916.0	-11.52
2F1	X034	13.4	24.8	748.8	830.2	832.3	885.0	-52.73
3A1	S-2	94.5	498.8	839.2	841.4	866.3		
3A2	X051	67.7	214.2	783.5	792.6	835.9		
3B1	D	138.7	719.4	836.8	837.7	846.3	838.0	8.27
3B2	MK-2	81.7	740.1	939.1	931.9	919.0		
3C1	MK-2	80.5	731.5	939.6	933.7	910.9	937.0	-26.14
3C2	D	138.7	735.5	839.9	842.4	856.6		
3D1	S-1	94.5	477.7	833.3	835.8	850.9		
3D2	MK-2	80.5	740.8	942.7	934.0	918.9		
3F1	1/2D	138.7	377.8	771.9	776.9	823.7	791.0	32.70
3F2	D	138.7	753.0	843.2	843.2	856.6		
3F1	MK-2	80.5	742.9	943.3	935.5	909.9	901.0	8.88
3F2	MK-2	80.5	764.5	950.4	942.7	925.0		
4A1	X059	98.4	360.4	796.6	805.1	838.5		
4A2	D	101.8	701.1	881.7	878.5	867.4		
4A3	D	101.8	700.3	881.5	879.5	861.1		
4B1	D	101.8	670.9	873.9	872.8	861.9	863.0	-1.10
4B2	X012	58.2	291.9	832.4	838.8	861.3		
4B3	X027	34.1	234.6	881.4	881.0	904.9		
4C1	D	101.8	644.4	867.0	867.4	878.7		
4C2	X050	58.2	218.4	799.0	812.2	854.2		
4C3	X064	30.2	297.6	960.0	932.6	870.4	926.0	-55.64
4D1	D	101.8	642.3	866.5	865.7	863.3		
4D2	X043	81.7	534.8	872.8	873.1	877.8		
4D3	D	101.8	691.1	879.1	878.7	868.3		
4E1	X054	94.3	516.2	844.9	843.5	839.5	835.0	4.52
4E2	X018	13.4	22.4	744.0	805.5	837.1		
4E3	D	101.8	695.2	880.2	878.1	877.1		
4F1	X069	58.7	269.8	821.2	831.1	871.6	858.0	13.61
4F2	D	101.8	709.4	883.9	884.4	899.0		
4F3	D	101.8	706.6	883.2	882.0	887.2	874.0	13.24
5A1	C-7	67.1	398.1	856.5	857.5	856.0		

D-RF REPRESENTS A REDUCED FLOW DRIVER ELEMENT  
 D-CF REPRESENTS A CONTROLLED FLOW DRIVER ELEMENT

TABLE III. (contd)

CASE 1 RUN: 39A DATE: 3/23/71 TIME: 1741. HOURS TOTAL MEASURED POWER: 49756.3 KW  
 TOTAL COMPUTED POWER: 46596.0 KW COMPUTED POWER, ROWS 1-6: 44283.4 KW COMPUTED POWER, ROW 7: 2312.6 KW  
 TOTAL CALIBRATED FLOW: 6820.4 GPM CORE DIFFERENTIAL PRESSURE: 42.0

POSITION	EXPERIMENT	CALCULATED FLOW (GPM)	PFACOR POWER (IN KW)	COOLANT TEMPERATURE (TOP OF FUEL)	COOLANT TEMPERATURE (TOP OF BLANKET)	CALCULATED MIXED COOLANT TEMPERATURE	MEASURED COOLANT TEMPERATURE	DIFFERENCE BETWEEN MEASURED AND CALCULATED MIXED COOLANT TEMPERATURES
5A2	D	86.1	622.3	890.6	886.2	868.5		
5A3	C-8	67.1	419.3	864.4	867.1	865.4		
5A4	D	86.1	607.3	886.0	885.0	887.2	875.0	12.23
5B1	C-9	67.1	381.8	850.1	852.5			
5B2	X040	76.1	505.8	875.4	873.6			
5B3	C-10	67.1	410.1	861.2	862.3			
5B4	D	86.1	592.7	881.6	879.1			
5C1	C-11	67.1	350.1	841.5	842.8			
5C2	X065	71.6	461.9	870.2	866.8	868.4	876.0	-7.58
5C3	C-12	67.1	404.2	858.9	860.4	860.1		
5C4	D	86.1	581.8	878.2	876.9	871.2		
5D1	SSCR	14.7	11.7	722.1	782.4			
5D2	D	86.1	576.4	876.6	874.1			
5D3	C-2	67.1	405.8	859.5	860.1			
5D4	D	86.1	603.3	884.8	881.4			
5E1	C-3	67.1	376.4	847.9	851.4			
5E2	D	86.1	618.8	889.5	885.8			
5E3	C-4	67.1	428.4	868.4	868.1			
5E4	D	86.1	625.9	891.7	889.3			
5F1	C-5	67.1	395.9	855.6	857.8			
5F2	D	86.1	629.7	892.9	890.2	889.6		
5F3	XX01	33.2	171.5	836.2	847.1	881.8		
5F4	D	86.1	634.9	894.5	891.2	878.6		
6A1	D	74.4	471.5	867.2	862.1			
6A2	D	74.4	519.1	884.1	877.3	863.8		
6A3	D	74.4	538.9	891.1	885.3	873.1		
6A4	X055	33.9	278.8	917.0	895.4			
6A5	D	74.4	499.4	877.1	871.6			
6B1	D	74.4	445.4	858.0	853.3			
6B2	D	74.4	487.7	873.0	867.3			
6B3	D	74.4	512.1	881.6	875.7			
6B4	D	74.4	500.7	877.6	873.0			
6B5	X028	47.5	155.0	786.0	794.1			
6C1	D	74.4	423.2	850.1	844.6			
6C2	D	74.4	467.6	865.8	861.9			
6C3	X073	30.7	232.9	854.7	849.6			
6C4	D	74.4	491.5	874.3	868.6	865.4	888.0	-22.61
6C5	D	74.4	474.2	868.2	861.2			
6D1	D	74.4	419.8	848.9	843.4			

D-RF REPRESENTS A REDUCED FLOW DRIVER ELEMENT  
 D-CT REPRESENTS A CONTROLLED FLOW DRIVER ELEMENT

TABLE III. (contd)

CASE 1 RUN: 39A DATE: 3/23/71 TIME: 1741. HOURS TOTAL MEASURED POWER: 49756.3 KW  
 TOTAL COMPUTED POWER: 46596.0 KW COMPUTED POWER, ROWS 1-6: 44283.4 KW COMPUTED POWER, ROW 7: 2312.6 KW  
 TOTAL CALIBRATED FLOW: 6820.4 GPM CORE DIFFERENTIAL PRESSURE: 42.0

POSITION	EXPERIMENT	CALCULATED FLOW (GPM)	REACTOR POWER (IN KW)	COOLANT TEMPERATURE (TOP OF FUEL)	COOLANT TEMPERATURE (TOP OF BLANKET)	CALCULATED MIXED COOLANT TEMPERATURE	MEASURED COOLANT TEMPERATURE	DIFFERENCE BETWEEN MEASURED AND CALCULATED MIXED COOLANT TEMPERATURES
6D2	D	74.4	474.5	868.3	860.5			
6D3	D	74.4	505.1	879.2	873.8			
6D4	1/2D	74.4	268.2	795.1	801.5			
6D5	D	74.4	491.7	874.4	869.1			
6E1	D	74.4	447.2	858.6	857.0			
6E2	X072	26.9	234.3	930.7	904.9			
6E3	D	74.4	539.5	891.3	888.1			
6E4	D	74.4	528.9	891.1	887.2			
6E5	D	74.4	523.8	885.8	882.0			
6F1	X058	53.7	384.9	889.1	870.7			
6F2	D	74.4	524.6	886.1	882.3			
6F3	D	74.4	558.0	897.9	892.9	893.0		
6F4	D	74.4	557.7	897.8	890.7	882.3		
6F5	D	74.4	524.3	886.0	879.9			
7A1	B	22.4	50.2	759.2				
7A2	B	22.4	76.2	789.8				
7A3	X041	13.4	4.3	708.4				
7A4	B	22.4	93.0	809.7				
7A5	X061	12.9	3.1	706.3				
7A6	B	22.4	74.2	787.5				
7B1	XG04	18.2	20.3	729.3				
7B2	B	22.4	73.2	786.3				
7B3	X035	13.4	4.3	708.4				
7B4	B	22.4	89.1	805.0				
7B5	B	22.4	87.0	802.6				
7B6	B	22.4	71.4	784.3				
7C1	B	22.4	48.2	756.8				
7C2	B	22.4	71.0	783.7				
7C3	B	22.4	85.8	801.2				
7C4	B	22.4	87.3	803.0				
7C5	X038	13.4	4.3	708.4				
7C6	B	22.4	71.1	783.9				
7D1	XG03	17.9	19.1	728.1				
7D2	B	22.4	71.7	784.5				
7D3	B	22.4	87.3	803.0				
7D4	B	22.4	89.5	805.5				
7D5	B	22.4	88.6	804.4				
7D6	B	22.4	73.5	786.7				
7E1	X036	22.4	132.7	856.5				

D-RF REPRESENTS A REDUCED FLOW DRIVER ELEMENT  
 D-CF REPRESENTS A CONTROLLED FLOW DRIVER ELEMENT

TABLE III. (contd)

CASE 1    RUN: 39A    DATE: 3/23/71    TIME: 1741. HOURS    TOTAL MEASURED POWER: 49756.3 KW  
 TOTAL COMPUTED POWER: 46596.0 KW    COMPUTED POWER, ROWS 1-6: 44287.4 KW    COMPUTED POWER, ROW 7: 2312.6 KW  
 TOTAL CALIBRATED FLOW: 6370.4 GPM    CORE DIFFERENTIAL PRESSURE: 42.0

POSITION	EXPERIMENT	CALCULATED FLOW (GPM)	REACTOR POWER (IN KW)	COOLANT TEMPERATURE (TOP OF FUEL)	COOLANT TEMPERATURE (TOP OF BLANKET)	CALCULATED MIXED COOLANT TEMPERATURE	MEASURED COOLANT TEMPERATURE	DIFFERENCE BETWEEN MEASURED AND CALCULATED MIXED COOLANT TEMPERATURES
7F2	B	22.4	74.6	788.0				
7E3	NI	1.3	5.7	811.8				
7F4	B	22.4	93.5	810.2				
7E5	B	22.4	92.5	809.1				
7E6	B	22.4	76.4	790.1				
7F1	B	22.4	50.3	759.3				
7F2	B	22.4	76.9	790.7				
7F3	B	22.4	93.7	810.6				
7F4	B	22.4	93.7	810.6				
7F5	X063	13.8	2.4	704.5				
7F6	B	22.4	76.8	790.5				

Table IV lists the calculated COOLTEMP flow correction factor, measured flow through the instrumented subassemblies, and measured pressure drop between pumps and plenum for runs 39A-45B. Table V shows how these values changed during the time when each instrumented subassembly was in the reactor. The relative changes for each run agree within 3%.

The absolute values of the measured pressure drop and the calculated COOLTEMP flow correction factor, however, are not in agreement. Several factors could cause this difference:

1. Actual outer-blanket flow is probably larger than the measured flow. Experiments have increased the net flow resistance in rows 1-7, while the flow resistance of the outer blanket, rows 8-16, has not changed. This effect could lower the flow correction factor by 1%. The lowest measured pressure drop is 18% less than the reference-design pressure drop; this 18% change is equivalent to a blanket-flow change of 4.25%. Since the blanket flow is 1200 gpm compared with 7200 gpm for rows 1-7, the flow in rows 1-7 changes only 0.71% if the total flow remains constant.

2. The relative pressure drop from row to row (in rows 1-7) has probably changed with the addition of experiments. Experimental-irradiation subassemblies are orificed for lower flow rates than standard driver subassemblies. To compensate for reactivity effects of the experiments, blanket subassemblies (low flow) in rows 6 and 7 are replaced with driver subassemblies (higher flow). This not only increases the flow in the outer rows (6 and 7), but also probably decreases the variation in pressure drop from row to row (in rows 1-7). The effect would be a decrease in the flow correction factor for the outer rows (6 and 7).

(The local effects of flow variation, referred to in Sec. IIA, are to be measured in the 0.6-scale flow model.)

3. Actual total flow may be somewhat lower than shown by measurement. Burnup measurements on driver fuel suggest that the actual reactor power may be somewhat lower than indicated. (This implication is within the framework of uncertainties in performing burnup measurements.) This implies that the reactor coolant flowmeter possibly indicates somewhat higher than actual total flow. A lower total flow would, in effect, reduce the flow correction factor for all rows treated by the code. However, the temperature calculation is not affected, because power change and flow change have compensating effects.

TABLE IV. Flow Correction Factor, Measured Instrumented-subassembly  
Flow, and Pressure Drop: Runs 39A-45B

Run No.	COOLTEMP Flow Correction Factor	No. of Instrumented Subassembly	Instrumented- subassembly Flow, <sup>a</sup> gpm at 800°F	$\Delta P$ between Pump and Upper Plenum, <sup>b</sup> psi
39A	1.12	XX01	29.7	42.0
39B	1.15	XX01	30.0	43.4
40A	1.12	XX01	29.6	41.8
41A	1.10	XX01	29.3	41.7
41B	1.10	XX01	29.7	41.7
42	1.12	XX02	52.8	43.1
43	1.09	XX02	51.5	41.7
44A	1.08	XX02	51.0	41.3
44B	1.06	XX02	50.5	40.8
45A	1.06	XX02	50.1	41.0
45B	1.04	XX02	49.2	39.4

<sup>a</sup>XX01 reference flow is 29.5 gpm at a  $\Delta P$  of 38.8 psi; XX02 reference flow is 53.0 gpm at a  $\Delta P$  of 38.8 psi.

<sup>b</sup>From readout of automatic data logger.

TABLE V. Change in Flow Correction Factor, Pressure Drop, and  
Instrumented-subassembly Flow

<u>Run Number</u>	<u>COOLTEMP Flow Correction Factor</u>	<u><math>\Delta P</math> between Pump and Upper Plenum</u>	<u>Instrumented- subassembly Flow</u>
<u>% Change Related to Run 39A (XX01 in reactor)</u>			
39A	0	0	0
39B	+2.2	+1.7	+1.1
40A	-0.6	-0.2	-0.2
41A	-1.7	-0.3	-1.4
41B	-1.8	-0.3	-4.3
<u>% Change Related to Run 42 (XX02 in reactor)</u>			
42	0	0	0
43	-3.3	-2.6	-2.5
44A	-3.9	-2.1	-3.4
44B	-5.3	-2.7	-4.4
45A	-5.7	-2.5	-5.1
45B	-7.2	-4.4	-6.8



B. Comparison with Results of Power Calculation with Other Codes

Two other computer codes, BURNUP and DOT, calculate power in each grid position. Table VI compares, for the run-39A reactor loading, the results from these two codes with those from COOLTEMP.

BURNUP uses the same flux distribution that is used for COOLTEMP. For the run-39A loading, the data obtained experimentally by foil irradiation in run-29 were used. The experimental data were modified for flux tilt as described in Sec. II.B. DOT calculates the flux distribution based on transport theory. For DOT and COOLTEMP, 89% of the full power of 50 MWt is assumed to be generated in the first six rows; for BURNUP, 96.68% of the 50 MWt is assumed to be generated in the first eight rows. BURNUP and DOT consider gamma heating as a part of the fission-energy release. Gamma heating is a small part of the total heat production and is proportional to fission heat in fueled subassemblies. For structural experiments or experiments that contain a small amount of fissionable material as compared with the amount of structural material, gamma heat is either the only heat produced or a larger portion of the total heat production than that for a standard driver fuel subassembly.

It can be seen in Table VI that the agreement is within 10%. The positions where zero power production is shown for BURNUP and DOT calculations are those containing experiments with no fissionable material.

C. Comparison of Calculated Temperatures with Temperatures Measured by Melt Wires

Melt-wire temperature monitors have been used to measure coolant temperatures at the outlet of subassemblies. These monitors are made up of fusible alloy wires 1/16 in. in diameter and 1/4 in. long mounted in 1/8-in.-dia holes in a bar which replaces one of the webs at the lower end of the subassembly top adapter. Each bar contains six melt wires (two each of three different melting points). A follower made of boron stainless steel rests on the top of each wire. When a wire melts, its follower drops down. The change in position of the follower is observed by neutron radiographs (see Fig. 3) taken before and after irradiation. The maximum temperature reached

TABLE VI. Power (kW) in Subassemblies in Rows 1-6 in EBR-II  
Run 39A, as Calculated by Three Codes

<u>Grid Position</u>	<u>COOLTEMP</u>	<u>DOT</u>	<u>BURNUP</u>
1A1	786.6	782.0	776.1
2A1	773.7	763.0	763.8
2B1	20.7	0	0
2C1	766.8	782.2	773.2
2D1	24.5	0	0
2E1	768.7	760.9	762.9
2F1	24.8	0	0
3A1	498.8	496.8	497.7
3B1	719.8	716.6	722.4
3C1	731.5	749.9	746.7
3D1	477.7	477.8	483.1
3E1	377.8	367.5	371.3
3F1	742.9	762.8	757.1
3A2	214.2	222.4	200.8
3B2	740.1	750.3	754.8
3C2	735.5	724.9	742.3
3D2	740.8	752.4	756.3
3E2	753.0	756.6	759.3
3F2	764.5	801.4	779.2
4A1	360.4	390.7	362.2
4B1	670.9	676.1	664.1
4C1	644.4	644.1	648.8
4D1	642.3	650.7	647.5
4E1	516.2	546.1	535.5
4F1	269.8	265.8	262.1
4A2	701.1	700.4	700.3
4B2	291.9	282.1	274.9
4C2	218.4	218.8	220.6
4D2	534.8	572.9	555.6
4E2	22.4	0	0
4F2	709.4	722.4	706.0
4A3	700.3	701.0	704.5
4B3	234.6	235.5	233.2
4C3	297.6	294.5	295.5
4D3	691.1	696.5	694.6
4E3	695.2	710.4	700.0
4F3	706.6	717.9	710.7
5A1	398.1	396.1	379.5
5B1	381.8	382.9	364.1
5C1	360.1	354.9	344.0
5D1	11.7	0	0
5E1	376.4	362.3	360.1
5F1	395.9	389.1	378.2
5A2	622.3	634.5	623.1
5B2	505.8	550.7	523.1

Table VI (contd)

<u>Grid Position</u>	<u>COOLTEMP</u>	<u>DOT</u>	<u>BURNUP</u>
5C2	461.9	501.2	479.9
5D2	576.4	589.4	579.6
5E2	618.8	610.8	622.1
5F2	629.7	631.7	631.3
5A3	418.3	405.2	399.8
5B3	410.1	402.4	392.9
5C3	404.2	399.4	388.1
5D3	408.8	403.8	389.7
5E3	428.4	416.9	411.0
5F3	171.5	141.6	158.5
5A4	607.3	604.2	608.2
5B4	592.7	589.8	595.0
5C4	581.8	588.8	585.1
5D4	603.3	612.5	607.0
5E4	625.9	625.0	628.5
5F4	634.9	633.6	636.2
6A1	471.5	469.2	465.8
6B1	445.4	434.8	440.2
6C1	423.2	407.8	409.9
6D1	419.8	427.6	417.4
6E1	447.2	426.8	444.8
6F1	384.9	392.6	397.7
6A2	519.1	519.6	515.4
6B2	487.7	483.3	484.6
6C2	467.6	472.3	465.9
6D2	474.5	473.6	474.2
6E2	234.8	235.5	229.4
6F2	524.6	511.6	526.2
6A3	538.9	535.5	536.3
6B3	512.1	511.2	510.2
6C3	232.9	239.1	229.4
6D3	505.1	508.4	505.9
6E3	539.5	529.6	539.5
6F3	558.0	542.5	549.4
6A4	278.8	276.1	278.0
6B4	500.7	502.7	499.1
6C4	491.5	500.8	491.6
6D4	268.2	252.3	260.4
6E4	538.9	527.3	538.4
6F4	557.7	549.5	555.8
6A5	499.4	488.3	495.2
6B5	155.0	151.7	152.2
6C5	474.2	480.1	473.7
6D5	491.7	482.2	492.2
6E5	523.8	510.4	522.2
6F5	524.3	520.8	521.0
Total	44,283.0	44,274.4	44,080.6

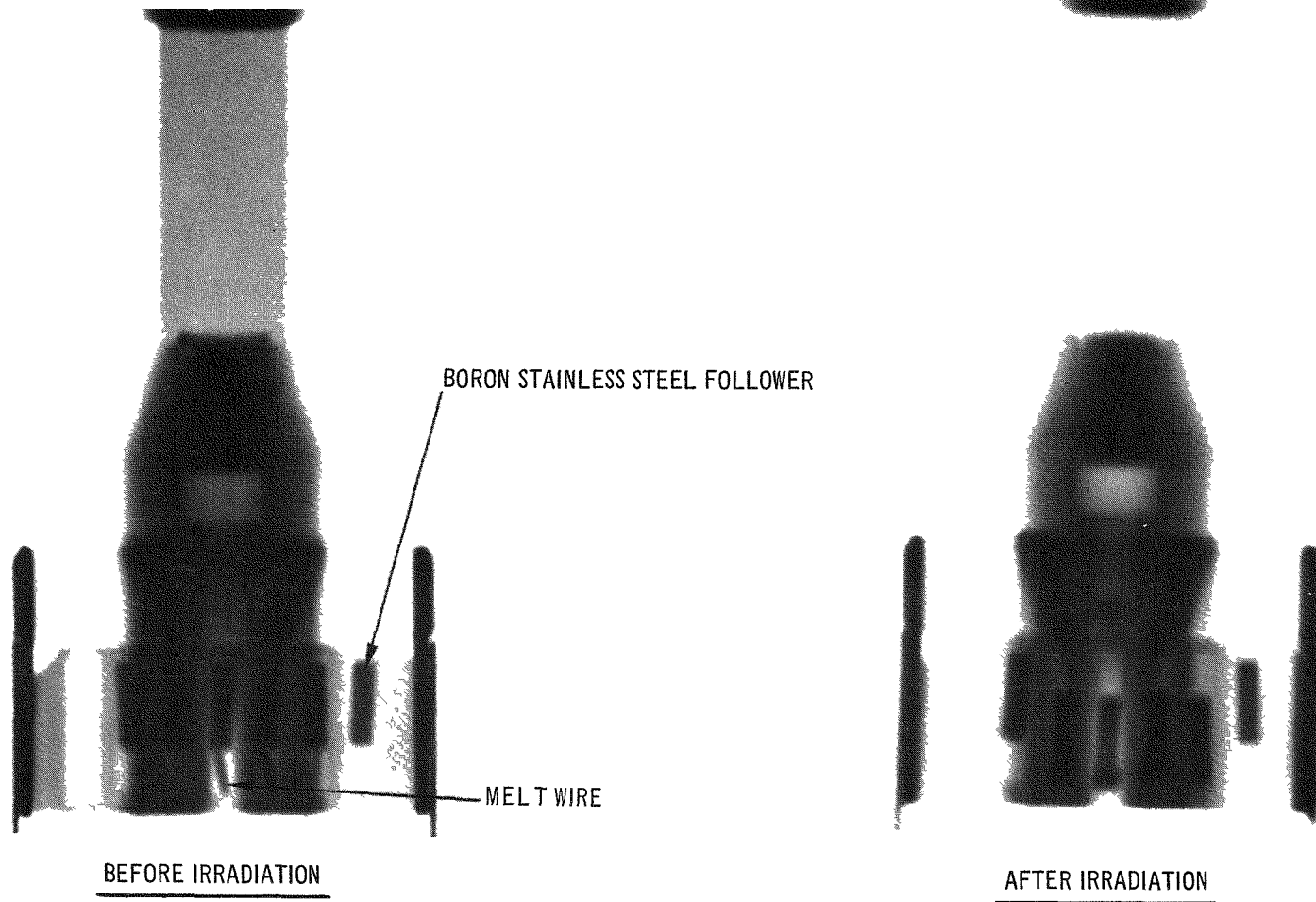


Fig. 3. Neutron Radiographs of Melt-wire Temperature Monitor before and after Irradiation;  
the Four Center Wires Melted during Irradiation

by the device lies somewhere between the melting point of the melted wire with the highest melting point and that of the unmelted wire with the next highest melting point.

Table VII gives the results of these measurements and compares them with the top-of-reflector temperatures calculated by COOLTEMP. The temperatures measured by melt wires are shown by using the symbols > (for the wire melted) and < (for the wire not melted); actual temperature lies between these values. For positions 4B1 (at 62.5 MWt) and 5A4, the highest melting point of the wires used was 926°F. One of the two wires with this melting point had partially melted. It is therefore believed that the actual temperature was very near 926°F.

The temperatures measured by the melt wires should correspond to the calculated top-of-reflector temperatures. Heat generated in the melt wires and their followers by absorption of gamma energy could have caused the wires to melt at a lower-than-rated temperature. Or, of course, the difference between the measured and calculated temperatures could be due to slight inaccuracies in the COOLTEMP code.

D. Comparison of Calculated Temperatures with Temperatures Measured by Thermocouples

There are 19 thermocouples mounted above subassemblies in rows 1-6. Figures 4-22 compare temperatures measured by these thermocouples (see Fig. 2) in runs 30A-45B with those calculated by COOLTEMP. The calculated temperatures are the last three listed in the legend for the figures, i.e., Mixed Coolant, Top of Reflector, and Top of Fuel. (Mixed-coolant and top-of-reflector temperatures coincide for position 1A1, Fig. 4.) During this period, 50 MWt was full rated power; the values graphed are for this power.

For position 1A1, calculated and measured values are in good agreement. The mixing effect appears to increase the deviation between calculated and measured values in the later runs.

The coolant temperatures for position 2A1 rose to 900-950°F when reduced-flow subassemblies were installed. (The same is true for positions 2C1, 2E1, 3C1, 3E1, 3F1, 4B1, and 4C3.) It can be noted from Fig. 5 (for position 2A1) that the calculated and measured temperatures are in good agreement for run 31G. For the next run, 32A, a fueled driver subassembly

*(Text continues on p. 56)*

TABLE VII. Comparison of Calculated Top-of-reflector Temperatures with  
Temperatures Measured by Melt Wires

<u>Core Position</u>	<u>Power, MWt</u>	<u>Calculated Temperature,<sup>a</sup> °F</u>	<u>Measured Temperature, °F</u>	
1A1	50	834	>845	<890
2A1	50	829	>845	<890
2C1	50	835	>845	<890
3B1	50	845	>845	<890
3E1	50	844	>845	<890
4B1	50	880	>890	<926
4B1	62.5	921	>926 <sup>b</sup>	
5A4	50	894	>926 <sup>b</sup>	
6D1	50	865	>890	<926
6E4	50	886	>890	<926
6E5	50	878	>890	<926

---

<sup>a</sup> Subassemblies remained in the reactor for several runs; highest values are given.

<sup>b</sup> One melt wire with highest melting point (926°F) was partially melted.

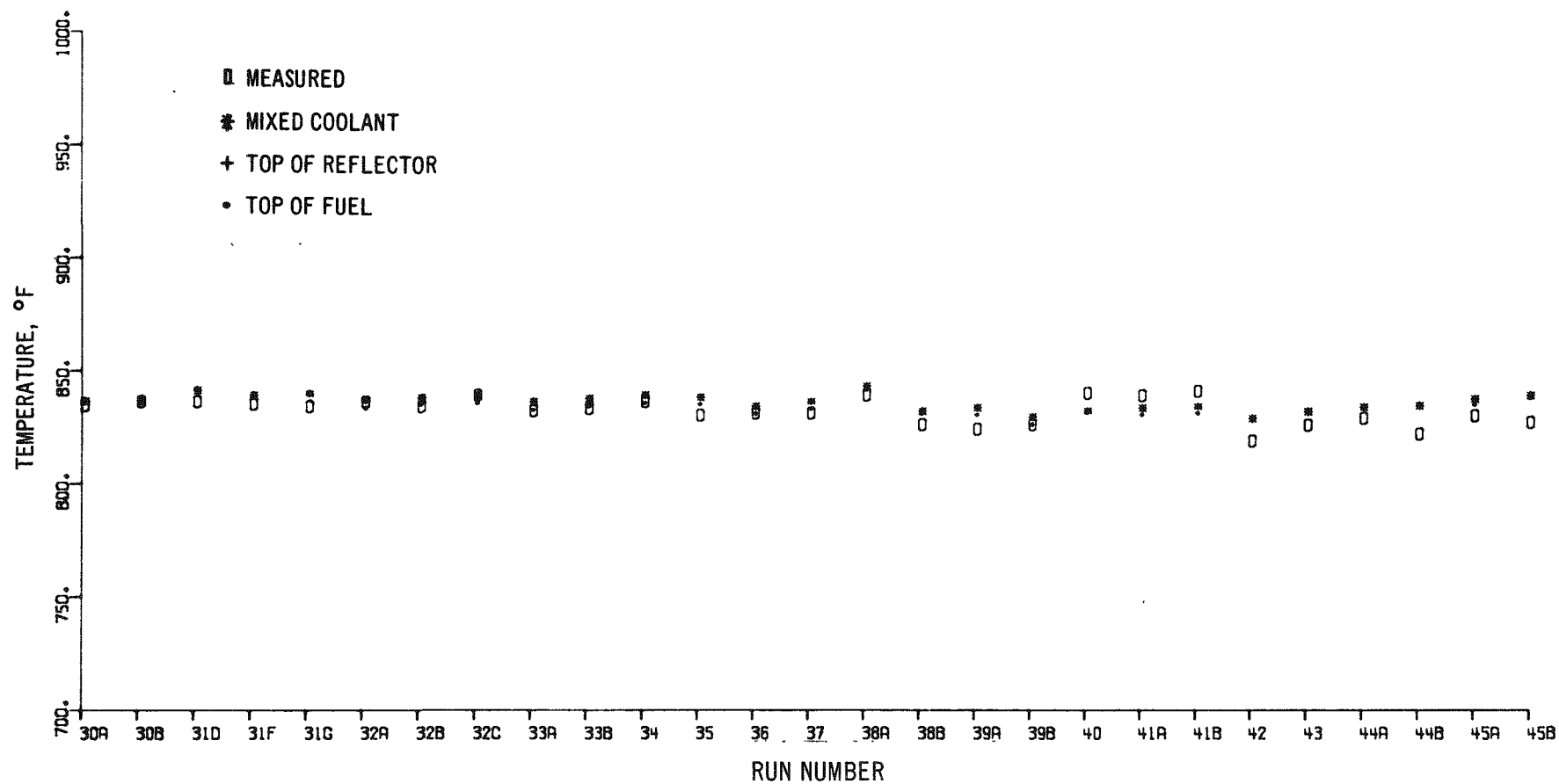


Fig. 4. Comparison of Thermocouple-measured and COOLTEMP-calculated Temperatures for Runs 30A-45B:  
Grid Position 1A1

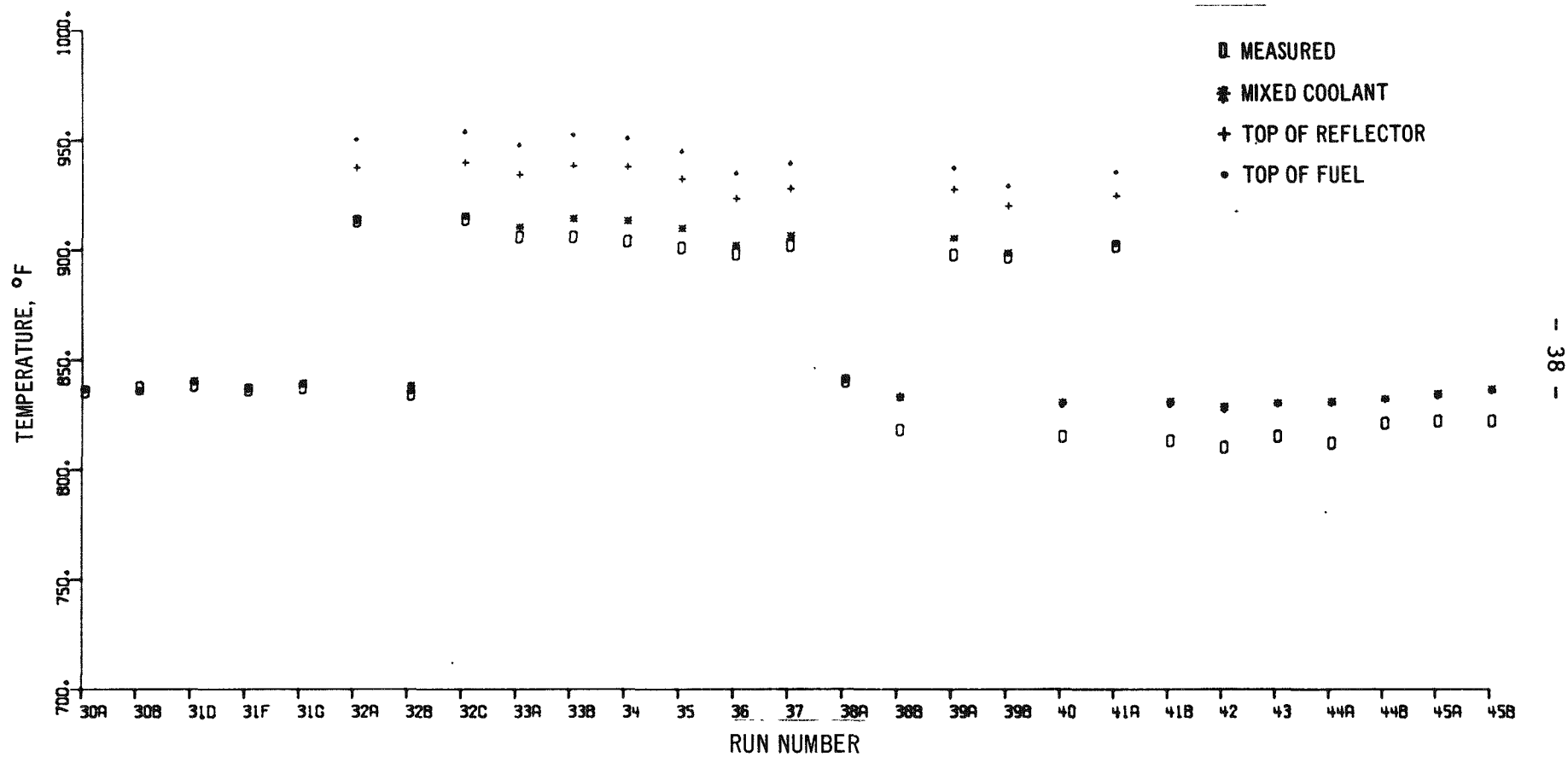


Fig. 5. Comparison of Thermocouple-measured and COOLTEMP-calculated Temperatures for Runs 30A-45B:  
Grid Position 2A1



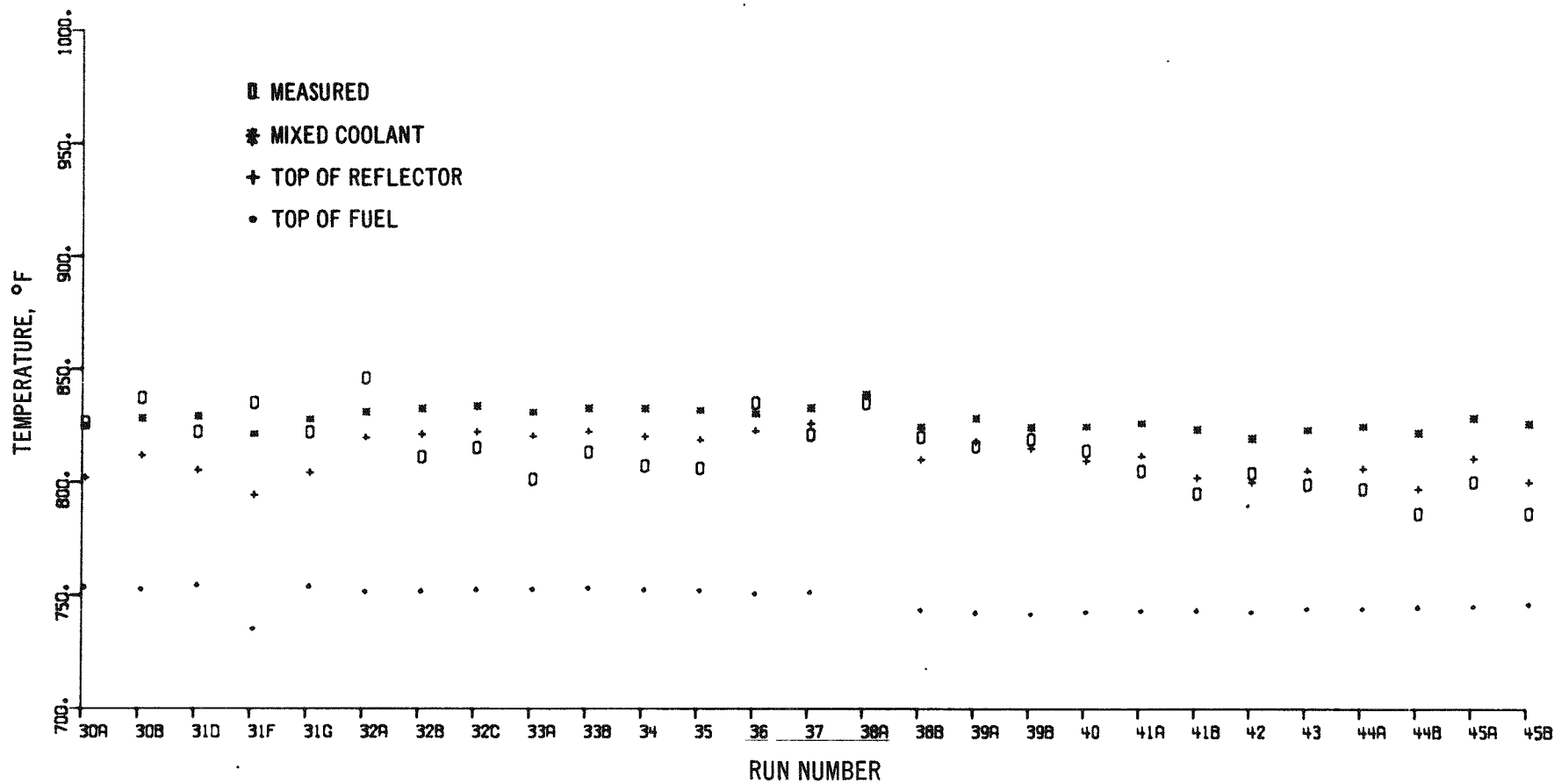


Fig. 6. Comparison of Thermocouple-measured and COOLTEMP-calculated Temperatures for Runs 30A-45B:  
Grid Position 2B1

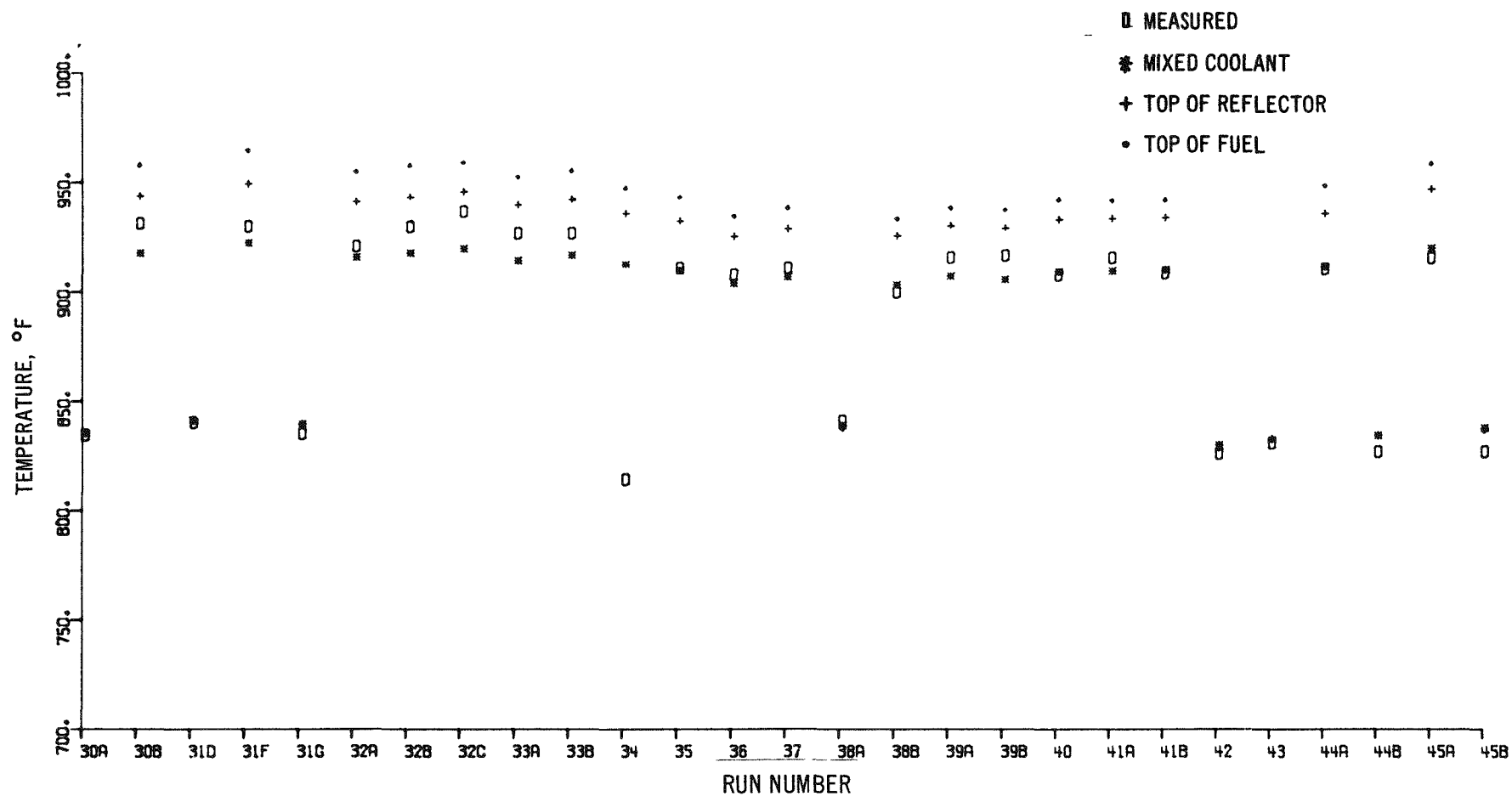


Fig. 7. Comparison of Thermocouple-measured and COOLTEMP-calculated Temperatures for Runs 30A-45B:  
Grid Position 2C1

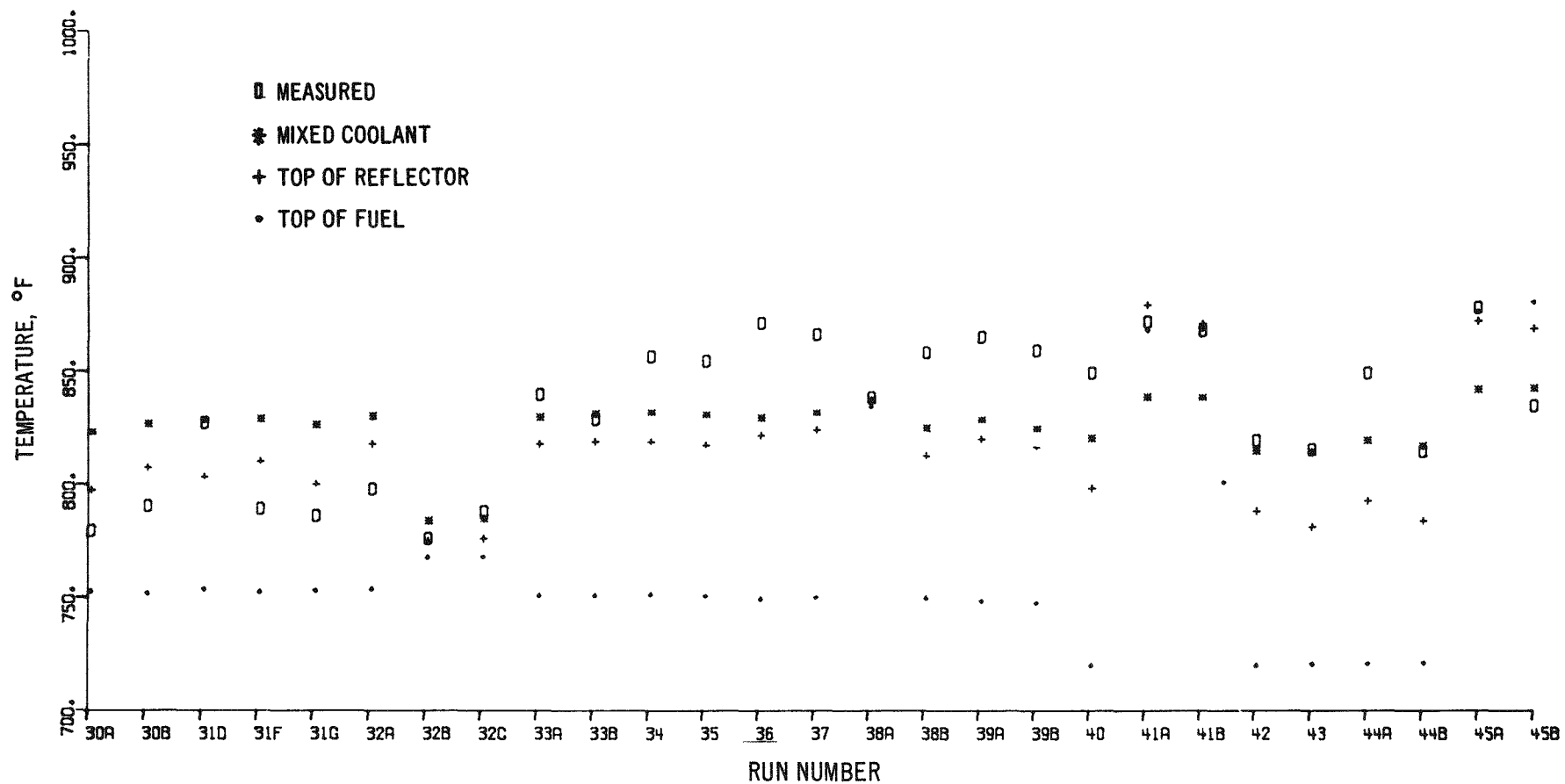


Fig. 8. Comparison of Thermocouple-measured and COOLTEMP-calculated Temperatures for Runs 30A-45B:

Grid Position 2D1

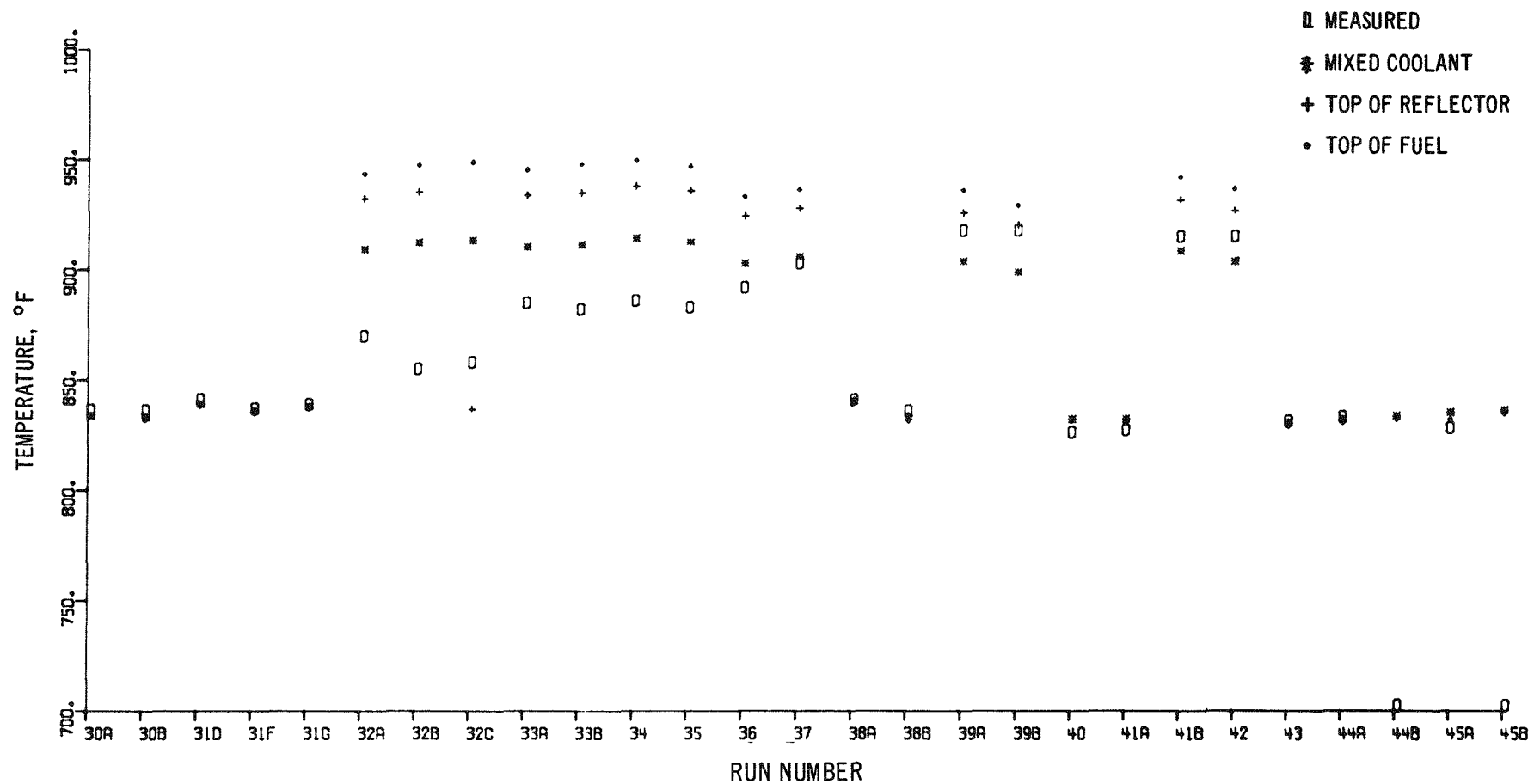


Fig. 9. Comparison of Thermocouple-measured and COOLTEMP-calculated Temperatures for Runs 30A-45B:  
Grid Position 2E1

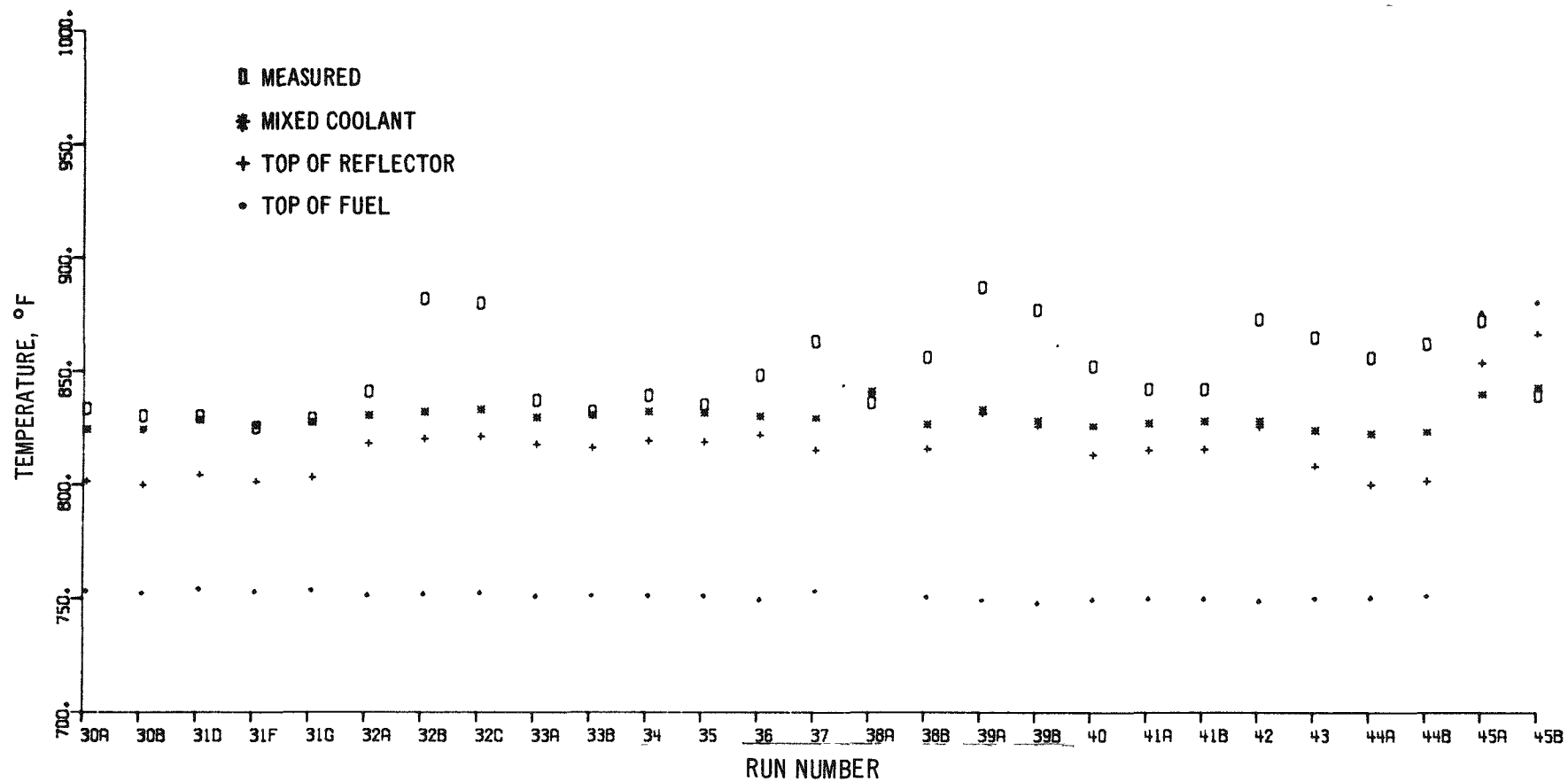


Fig. 10. Comparison of Thermocouple-measured and COOLTEMP-calculated Temperatures for Runs 30A-45B:  
Grid Position 2F1

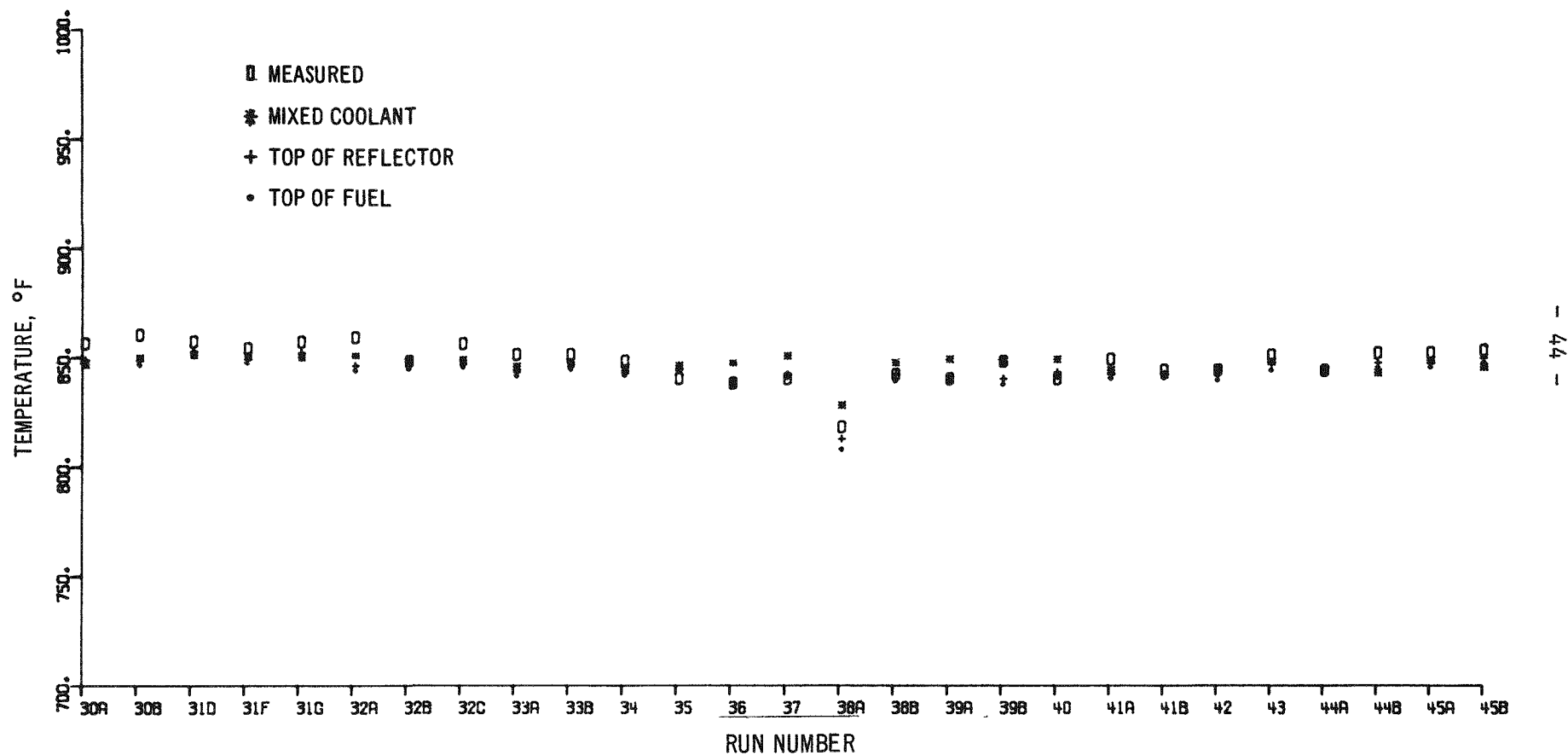


Fig. 11. Comparison of Thermocouple-measured and COOLTEMP-calculated Temperatures for Runs 30A-45B:  
Grid Position 3B1

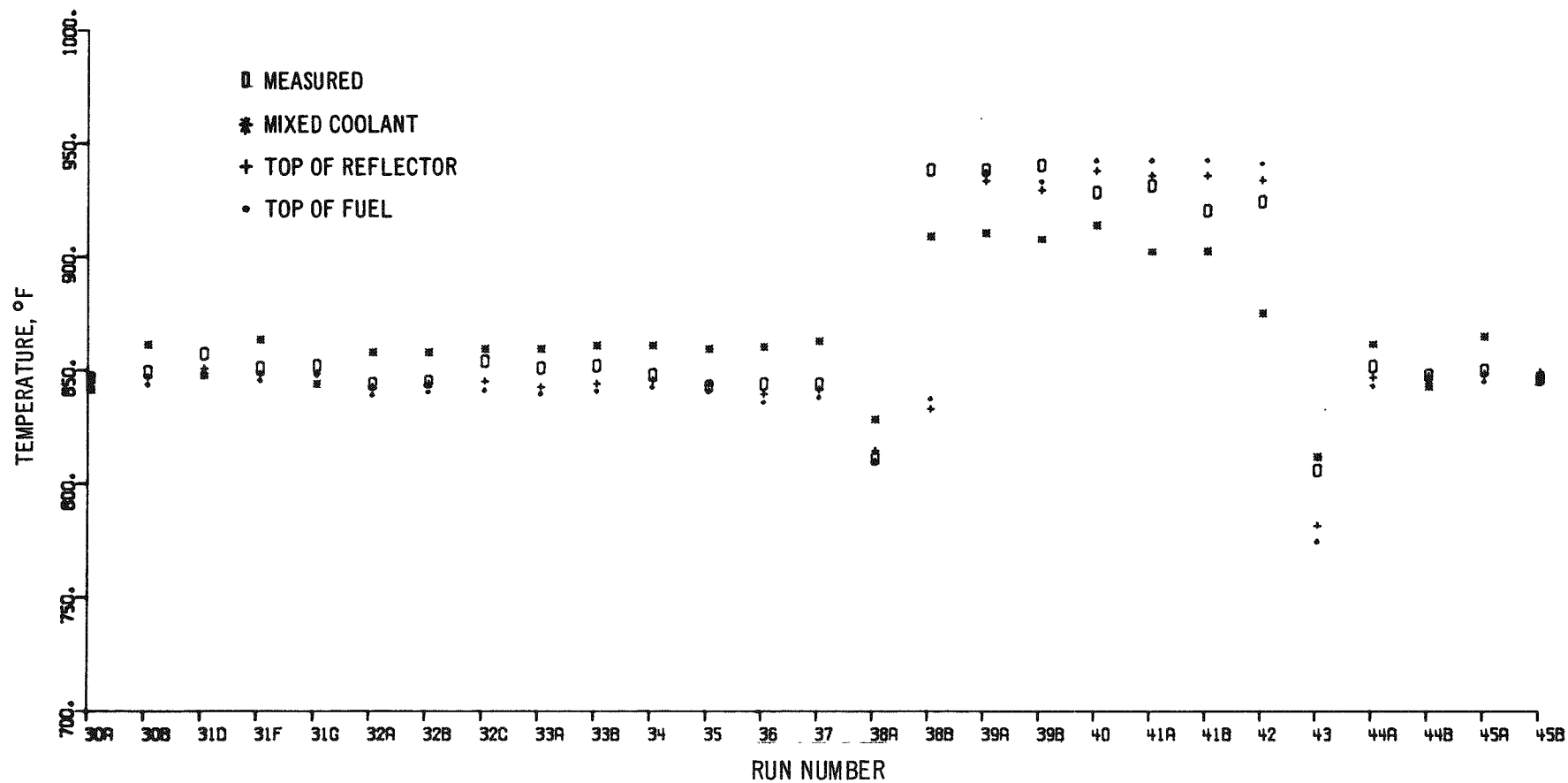


Fig. 12. Comparison of Thermocouple-measured and COOLTEMP-calculated Temperatures for Runs 30A-45B:

Grid Position 3C1

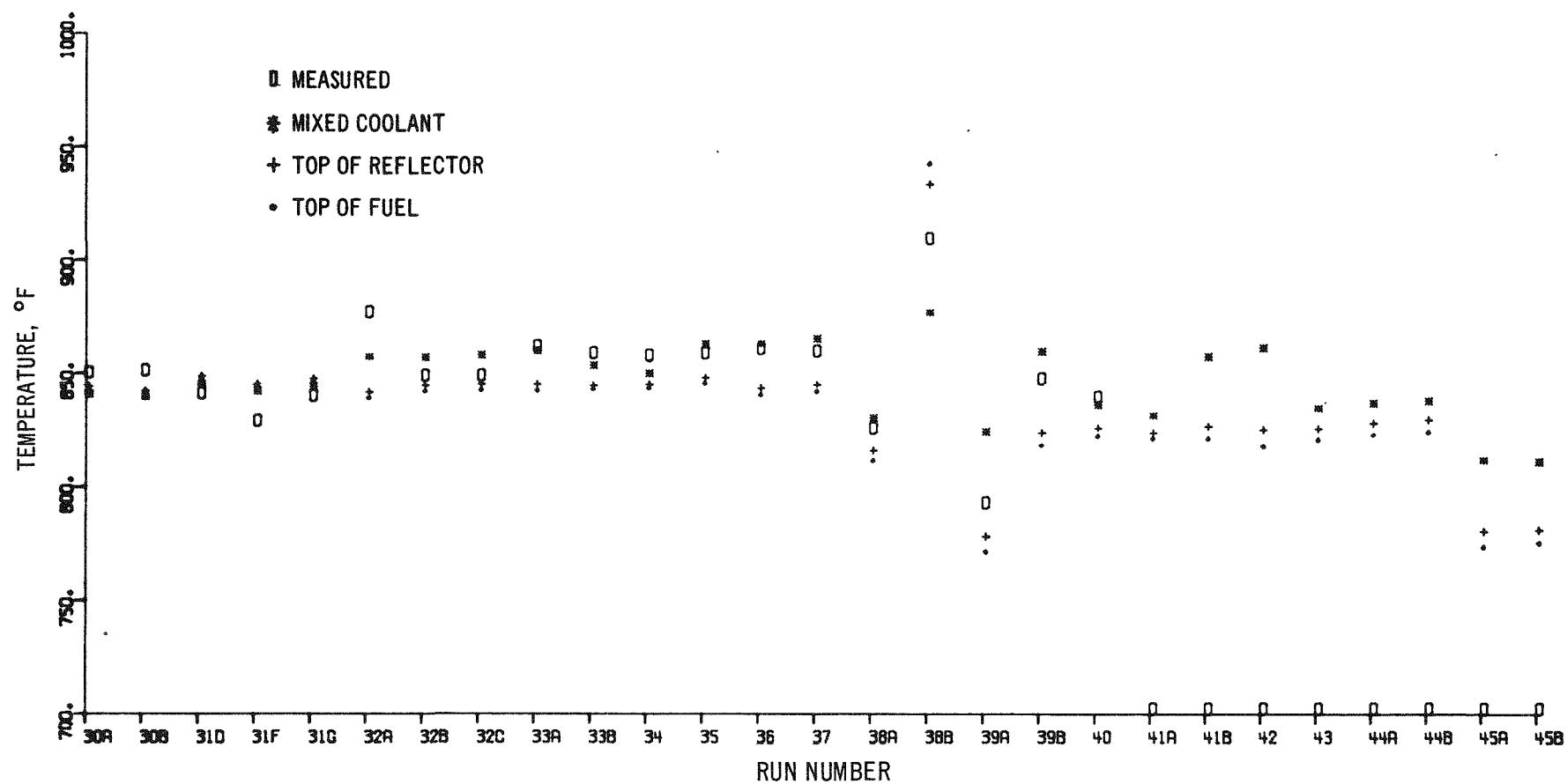


Fig. 13. Comparison of Thermocouple-measured and COOLTEMP-calculated Temperatures for Runs 30A-45B:  
Grid Position 3E1



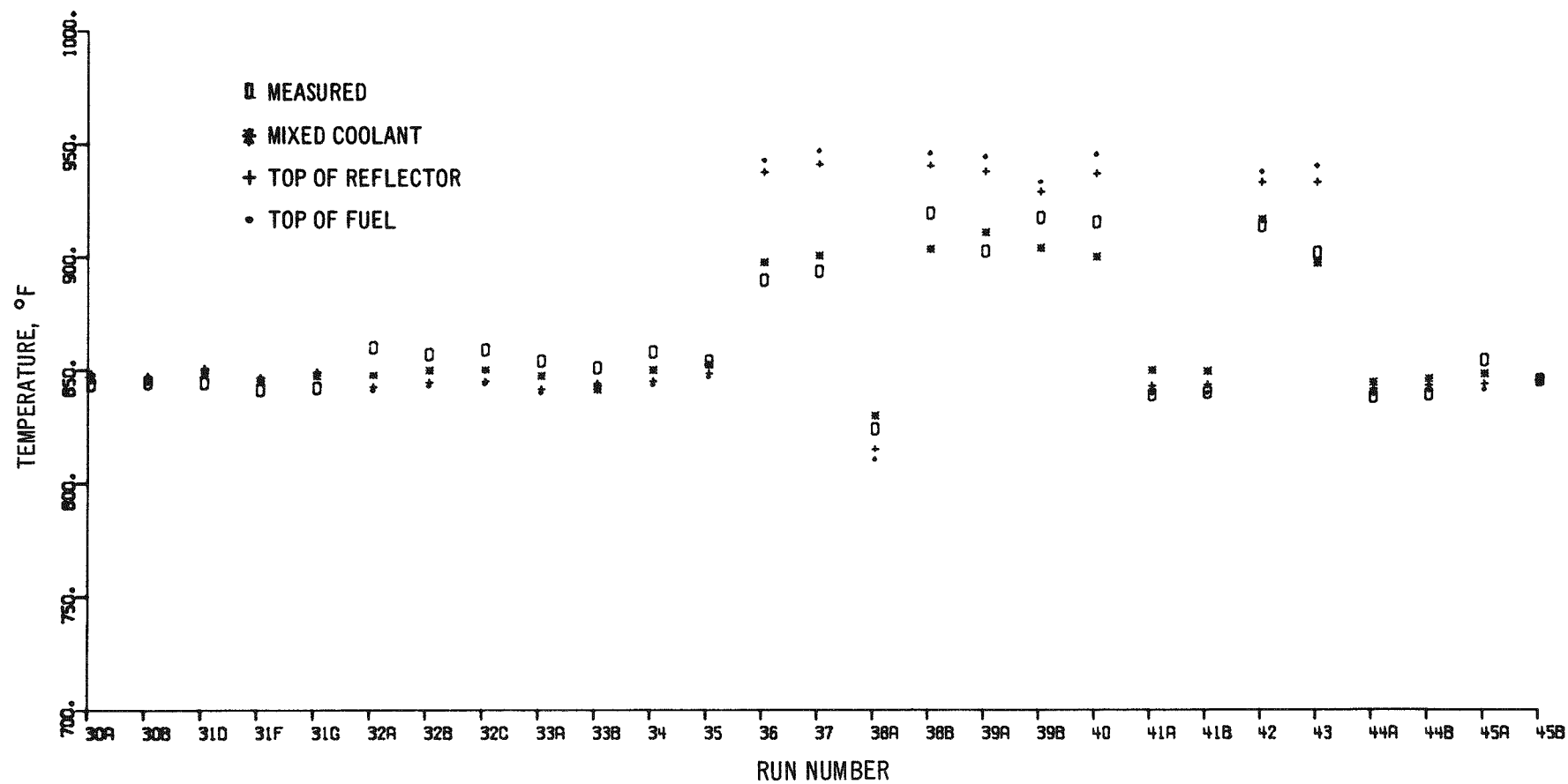


Fig. 14. Comparison of Thermocouple-measured and COOLTEMP-calculated Temperatures for Runs 30A-45B:  
Grid Position 3F1

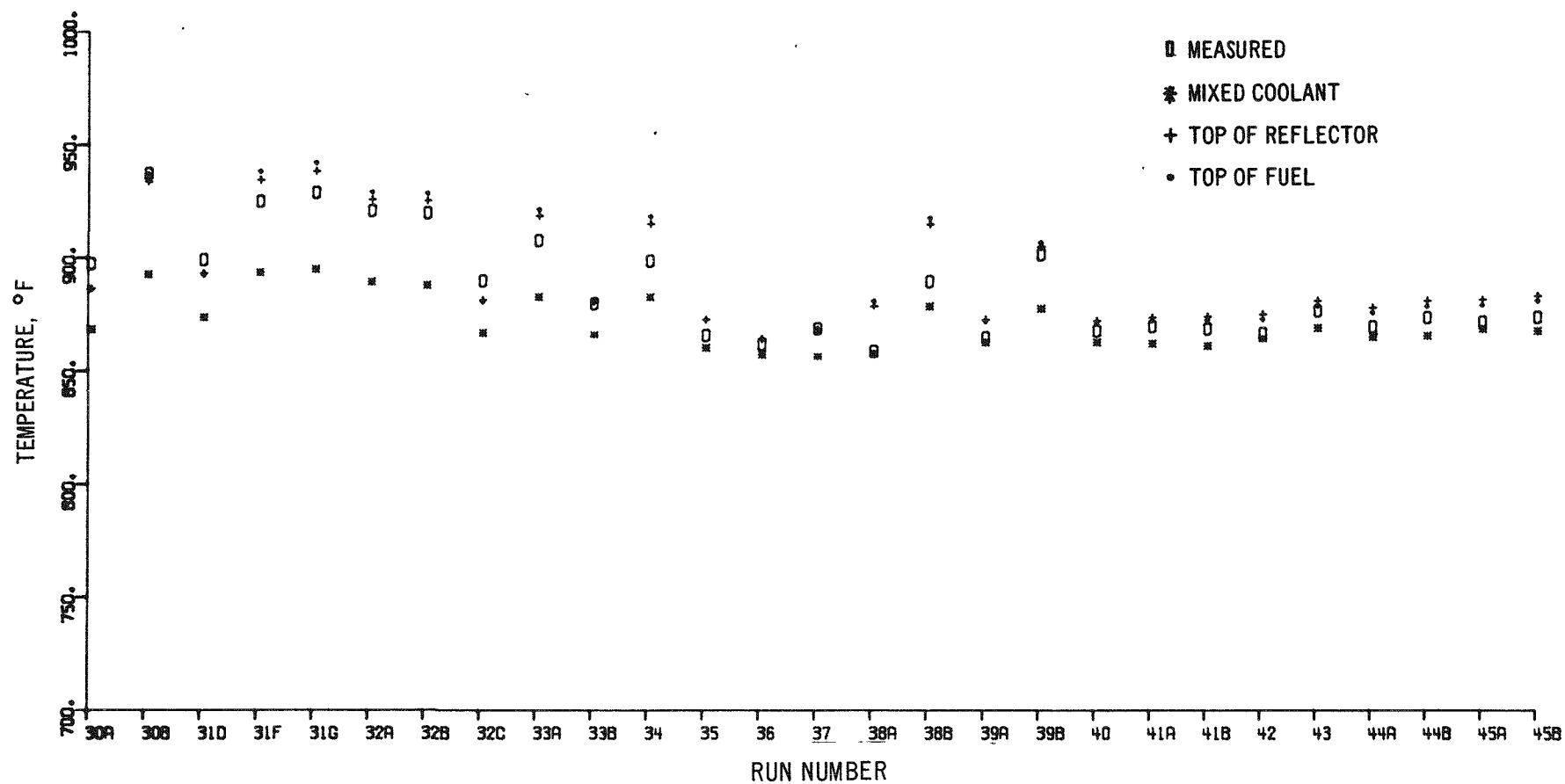


Fig. 15. Comparison of Thermocouple-measured and COOLTEMP-calculated Temperatures for Runs 30A-45B:  
Grid Position 4B1

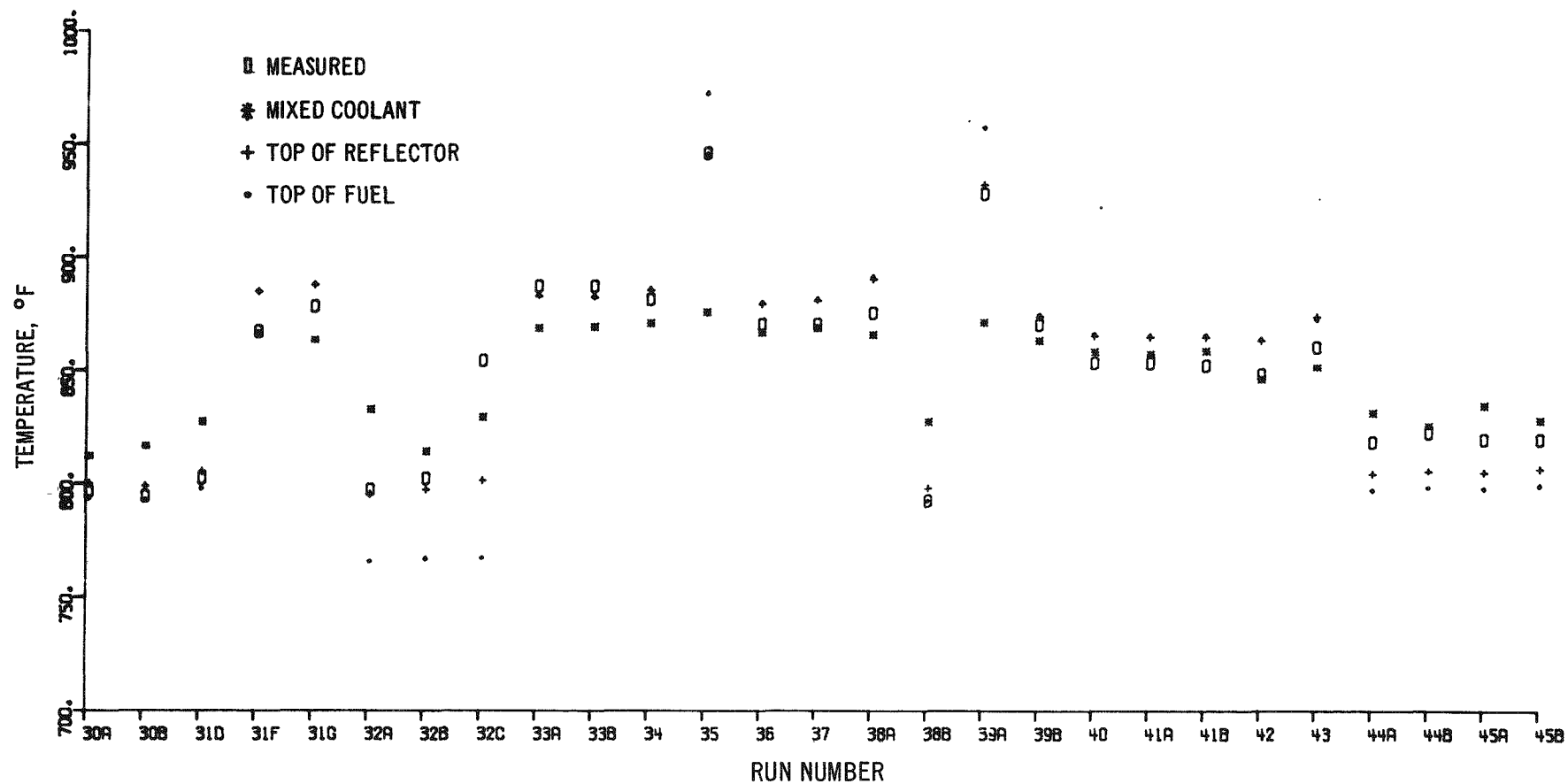


Fig. 16. Comparison of Thermocouple-measured and COOLTEMP-calculated Temperatures for Runs 30A-45B:

Grid Position 4C3

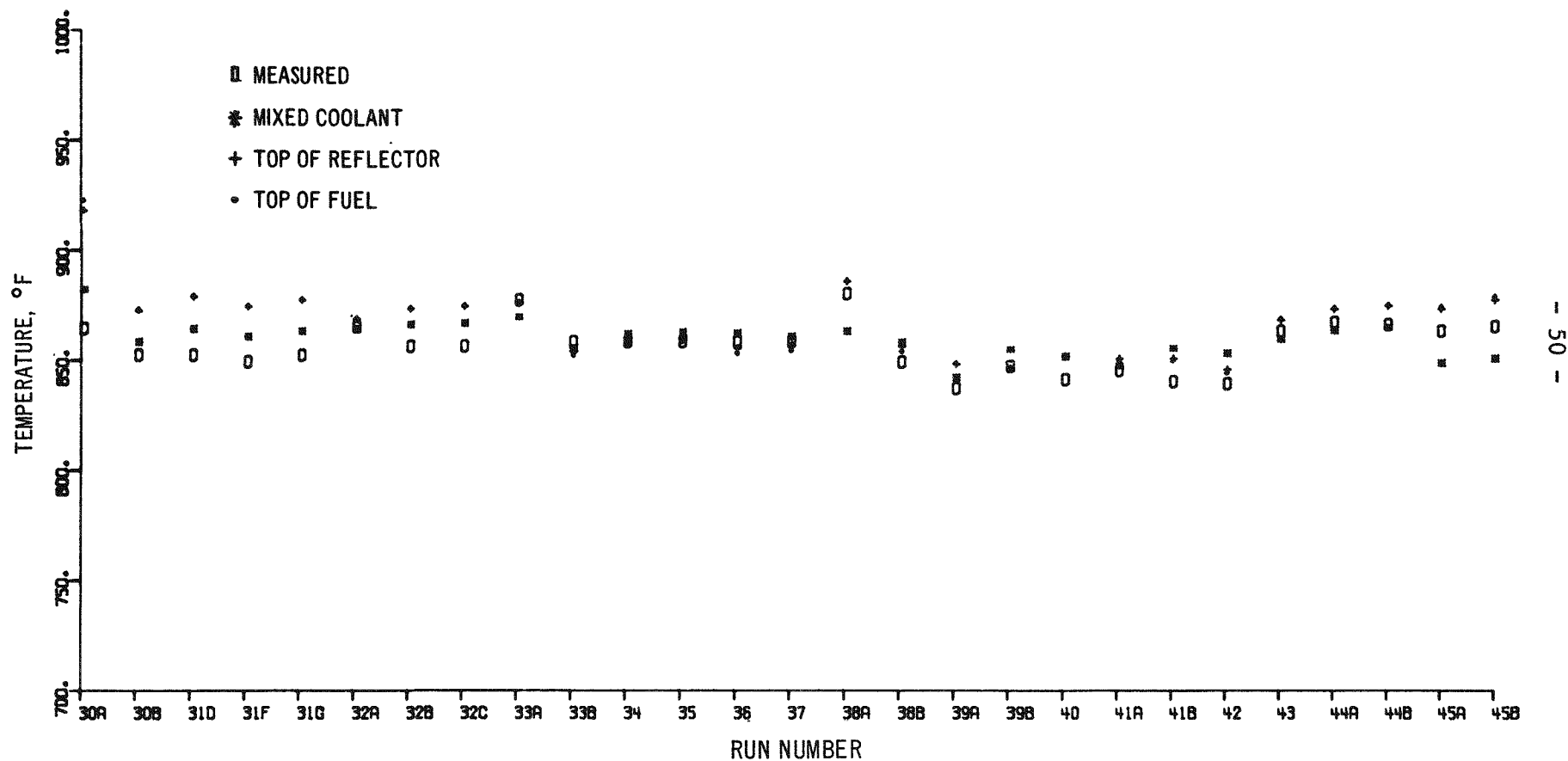


Fig. 17. Comparison of Thermocouple-measured and COOLTEMP-calculated Temperatures for Runs 30A-45B:  
Grid Position 4E1

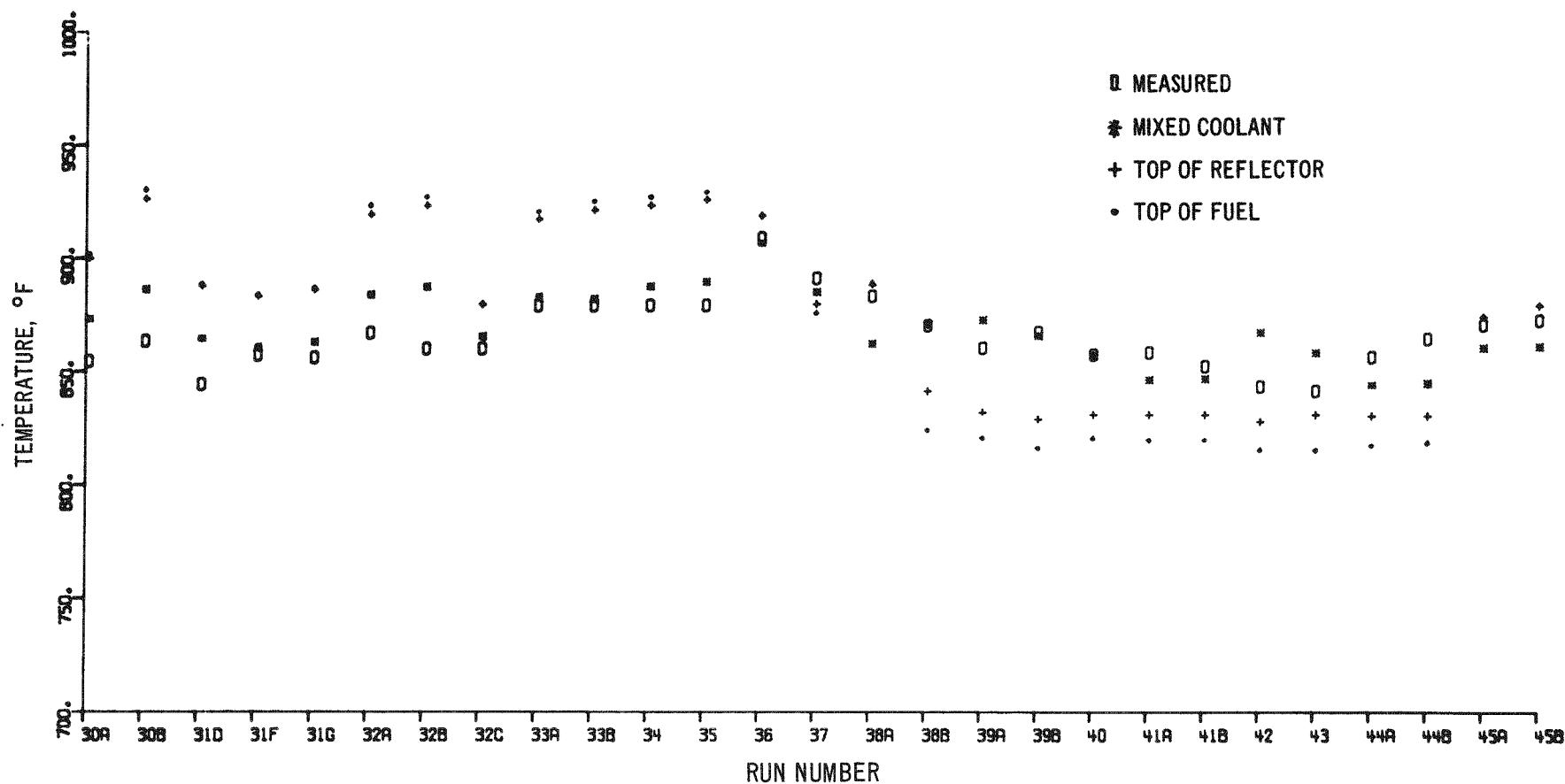


Fig. 18. Comparison of Thermocouple-measured and COOLTEMP-calculated Temperatures for Runs 30A-45B:  
Grid Position 4F1

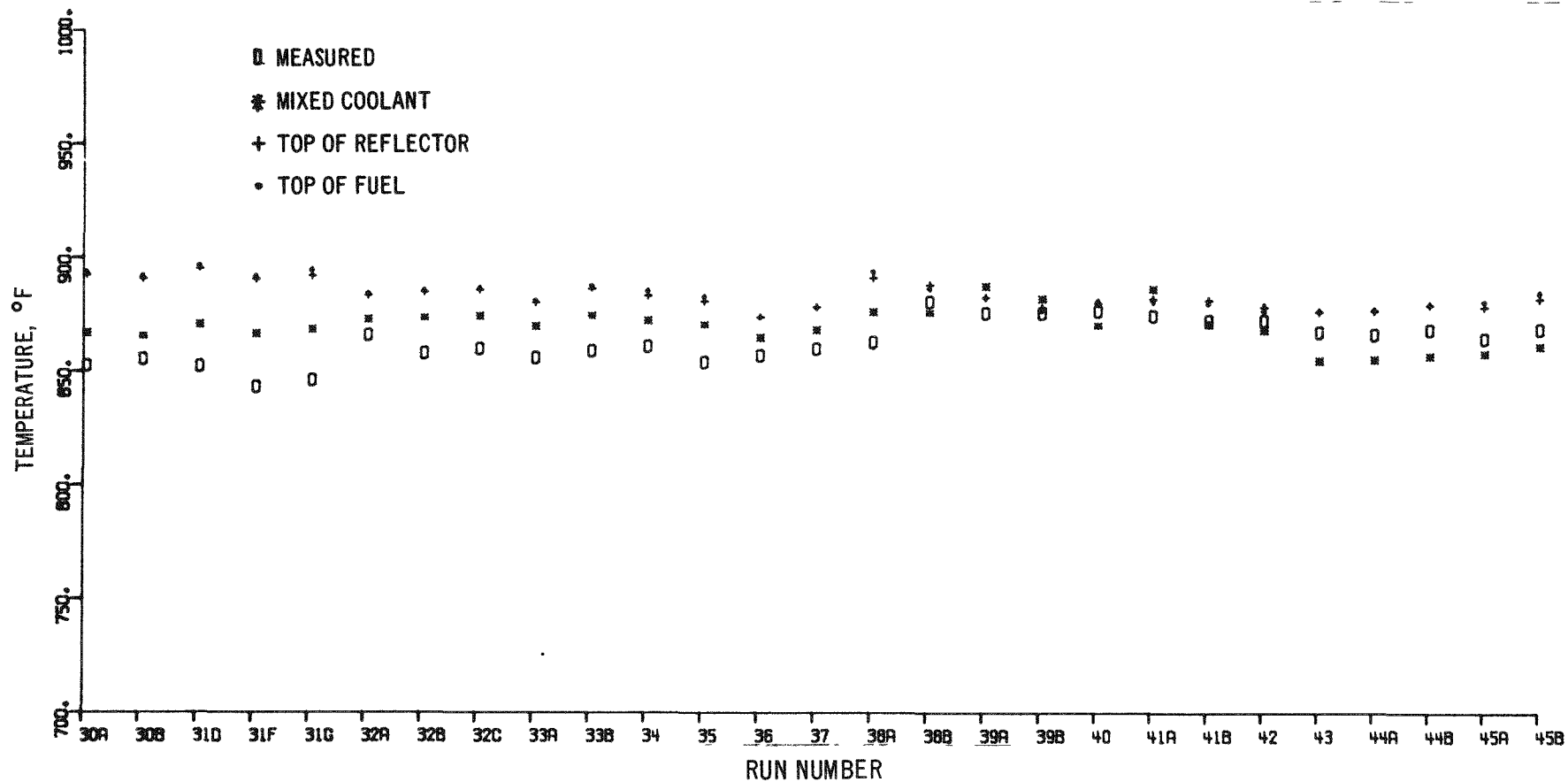


Fig. 19. Comparison of Thermocouple-measured and COOLTEMP-calculated Temperatures for Runs 30A-45B:  
Grid Position 4F3

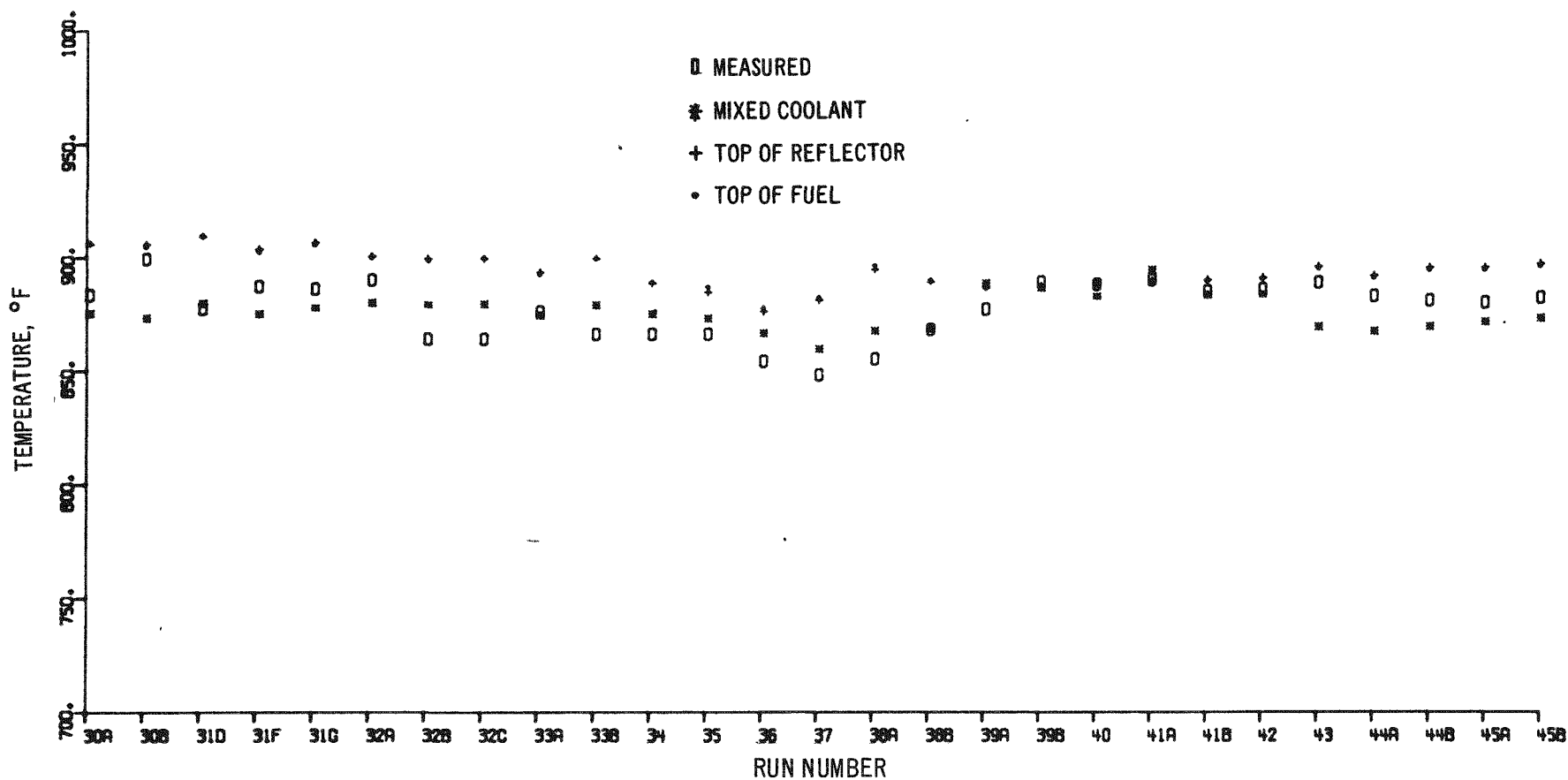


Fig. 20. Comparison of Thermocouple-measured and COOLTEMP-calculated Temperatures for Runs 30A-45B:  
Grid Position 5A4

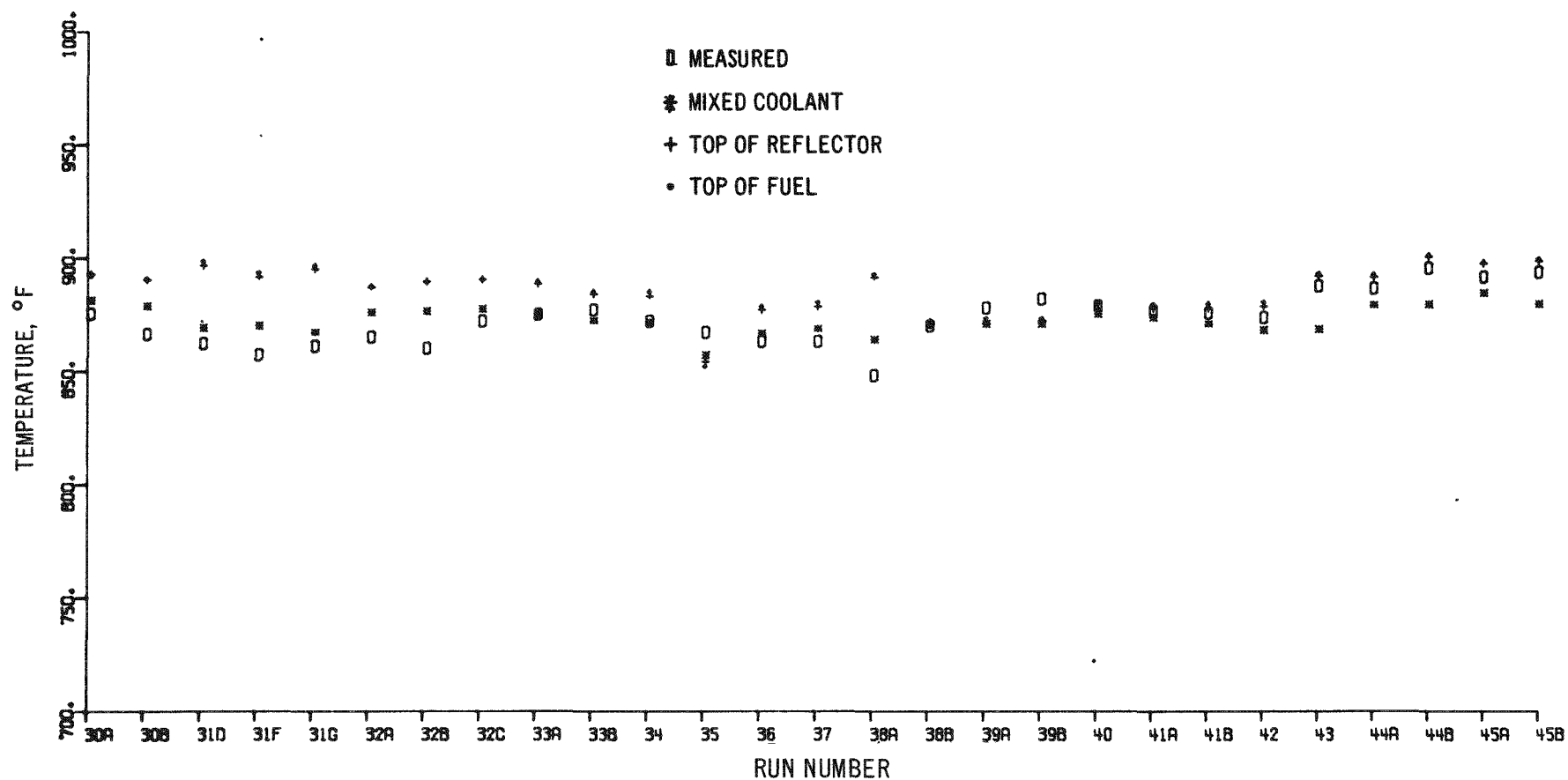


Fig. 21. Comparison of Thermocouple-measured and COOLTEMP-calculated Temperatures for Runs 30A-45B:  
Grid Position 5C2



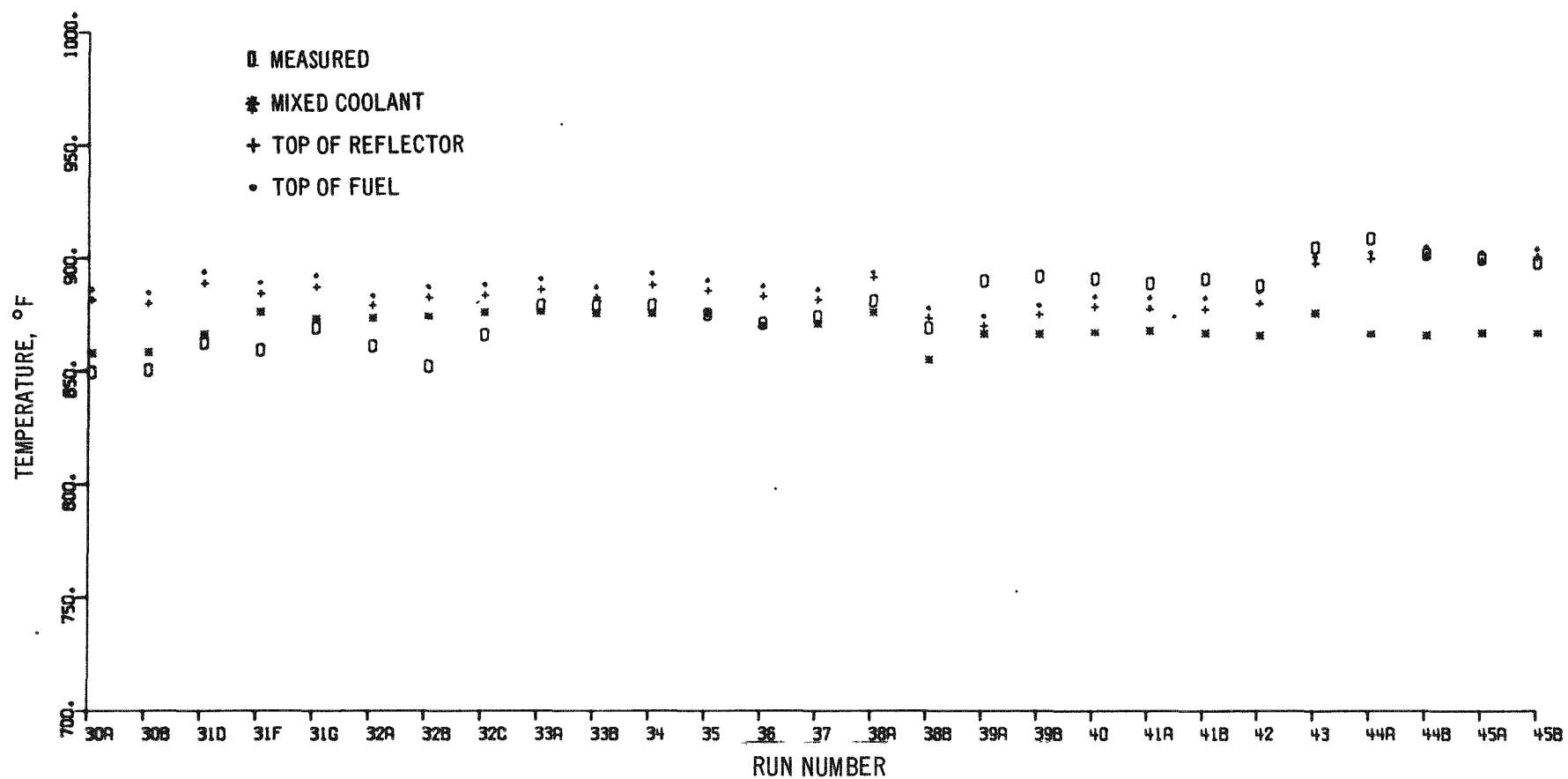


Fig. 22. Comparison of Thermocouple-measured and COOLTEMP-calculated Temperatures for Runs 30A-45B:

Grid Position 6C4

*(Text continued from p. 35)*

with 70% of normal flow causes 211°F temperature rise compared with 148°F for the previous run. Even with this large change, calculated and measured values are still in good agreement. The correction for the mixing effect improves the agreement between measured and calculated coolant temperatures.

For most runs, positions 2B1, 2D1, and 2F1 held experimental-irradiation subassemblies containing only structural materials (no fissionable material). It can be seen that the temperature rise due to radial heat transfer is greater than the rise due to heat production in these subassemblies. (The difference between the top-of-fuel temperature and 700°F is less than that between the top-of-reflector and top-of-fuel temperature.) The mixing correction in these cases usually does not improve agreement between calculated and measured temperatures.

The run-38A loading had standard driver subassemblies in all row-1 and row-2 positions. In this run, the measured and calculated values for these positions were in good agreement. Power and flow effects are apparently well represented for this loading in these positions.

For row-3 subassembly positions 3B1, 3C1, 3E1, and 3F1 (Figs. 11-14), agreement between calculated and measured values is good when standard driver subassemblies are installed. When top-of-fuel temperatures are outside the range of 820-850°F, reduced-flow subassemblies or experiments are operating in these positions, and differences between calculated and measured values are greater. The thermocouple for position 3E1 failed after run 41A. For the succeeding runs, 700°F was selected as the measured temperature merely for computer programming convenience.

The mixing effect is not completely represented by the model used. For most grid positions, however, it does improve the agreement between calculated and measured temperatures. Position 4B1 is an exception.

Although attempts have been made to reduce the difference between calculated and measured temperatures by accounting more precisely for the effects of flow, thermocouple location, etc., the desired goal of 10°F maximum difference has not been reached.

#### IV. CONCLUSIONS

COOLTEMP has provided useful information for several purposes. The results are not as accurate as one would like; however, efforts are being made to improve the accuracy. Improving the accuracy will require modification of the code as more analytical and experimental information becomes available.

Flow division between subassemblies, for example, is not accurately known. Data from the instrumented-subassembly flowmeter indicate that the COOLTEMP-calculated flows for this control-rod position were 12% higher than the measured values. However, changes in calculated flow, measured flow, and measured pressure drop corresponded within 3%. The relationships of flow to pressure drop measured in the 0.6-scale model are no longer valid, because the addition of experiments has changed the conditions.

Two factors cause difficulty in calculating expected measured temperatures. First, accuracy of calculations of subassembly outlet temperature are, in part, limited by uncertainties in the coolant flow. Second, location of the thermocouples in EBR-II does not allow measurement of performance of one subassembly only. Mixing of coolant streams from other subassemblies immediately after the coolant leaves a subassembly apparently has a significant effect on temperature measured by the subassembly-outlet-temperature thermocouples.